

DEC 20 1946

ARR No. E6C01

NATIONAL ADVISORY COMMITTEE FOR AERONAUTICS

WARTIME REPORT

ORIGINALLY ISSUED

March 1946 as
Advance Restricted Report E6C01

TEST-STAND INVESTIGATION OF COOLING CHARACTERISTICS

AND FACTORS AFFECTING TEMPERATURE DISTRIBUTION

OF A DOUBLE-ROW RADIAL AIRCRAFT ENGINE

By Michael A. Sipko, Robert O. Hickel
and Robert J. Jones

Aircraft Engine Research Laboratory
Cleveland, Ohio

NACA

WASHINGTON

NACA WARTIME REPORTS are reprints of papers originally issued to provide rapid distribution of advance research results to an authorized group requiring them for the war effort. They were previously held under a security status but are now unclassified. Some of these reports were not technically edited. All have been reproduced without change in order to expedite general distribution.

NACA ARR No. E5C01

NATIONAL ADVISORY COMMITTEE FOR AERONAUTICS

ADVANCE RESTRICTED REPORT

TEST-STAND INVESTIGATION OF COOLING CHARACTERISTICS

AND FACTORS AFFECTING TEMPERATURE DISTRIBUTION

OF A DOUBLE-ROW RADIAL AIRCRAFT ENGINE

By Michael A. Sipko, Robert O. Hickel
and Robert J. Jones

SUMMARY

Tests were conducted with a double-row radial, air-cooled engine to investigate the over-all cooling characteristics and to analyze to what extent variations in temperature distribution among the cylinders were caused by variations in cooling-air pressure drop, power, and fuel-air ratio. The tests of temperature distribution were made over a range of engine powers from 1000 to 1700 brake horsepower. The results also allowed estimation of the improvement in the cylinder-temperature pattern that might be attained through improvement in the distribution of cooling-air pressure drop, power, and fuel-air ratio.

The results indicate that a correlation of the over-all data and the individual cylinder data was possible; the slopes of the individual-cylinder correlation curves were the same but the levels varied. For the range of powers investigated, a direct correspondence was observed between the cylinder-temperature patterns and the distribution of cooling-air pressure drop, power, and fuel-air ratio although average temperature differences of 20° F were observed between the measured cylinder-head temperatures and those calculated from the individual-cylinder operating conditions. These temperature differences presumably result from uncontrollable and unaccountable variables and small variations in instrumentation. The variations in cylinder temperature that may be attained through improvement in the distribution of cooling-air pressure drop, power, and fuel-air ratio are of the same order as the difference between the observed and the calculated cylinder temperatures; that is, an average of approximately $\pm 20^{\circ}$ F.

INTRODUCTION

An air-cooled aircraft engine requires either an adequate flow of cooling air or a sufficiently enriched mixture to maintain the critical temperature regions of each cylinder below any value that might lead to engine failure. When the temperature differs greatly among the cylinders, this requirement is greatly increased and in turn the airplane performance is seriously restricted. In order to avoid these temperature differences, the causes of nonuniform temperature distribution, which may be nonuniform distribution of some of the operating variables among the cylinders, individual cylinder characteristics, or a combination of such variables and characteristics, must be determined.

The present investigation of the distribution of the cooling-air pressure drop, indicated horsepower, and fuel-air ratio among the cylinders was undertaken in an effort to determine the possible causes of nonuniform temperature distribution. A question exists, however, as to whether all temperature nonuniformity may be accounted for by variations in cooling-air pressure drop, power, and fuel-air ratio. Data from unpublished NACA tests have disclosed that a generally poor correspondence exists between the temperature and the operating conditions of each cylinder and also that, even when the difficulties of fuel-air-ratio distribution have been greatly relieved, through improved mixture distribution, a nonuniformity of cylinder temperature distribution still persists.

The average cooling performance of an air-cooled multicylinder engine is described by relating the average temperature of all the cylinders to the average cooling-air pressure drop, engine power, and over-all fuel-air ratio by means of a method introduced by Pinkel (reference 1). By this average relation, a change in one of the variables being investigated will show its effect upon the average temperature of all the cylinders.

A further refinement of the cooling performance can be made by determining the variation of cooling-air pressure drop, indicated horsepower, and fuel-air ratio among the cylinders and comparing the pertinent factors to the individual cylinder temperatures. By this method it can be observed how the individual cylinder operating conditions will cause the actual cylinder temperatures to vary from the average temperature of all the cylinders. In order to determine the amount by which the variations of cooling-air pressure drop, power, and fuel-air ratio will account for the variations in cylinder temperatures, the data for each cylinder were correlated and a comparison was made between the observed cylinder temperatures and the calculated cylinder temperatures.

Detailed tests were undertaken at the NACA Cleveland laboratory with a double-row air-cooled engine installed in a test stand in order to investigate the individual cylinder temperatures of a multi-cylinder engine as well as the relation of the average temperature of all cylinders to the engine operating conditions. From the analysis of these test data the magnitude of the temperature differences as well as the reduction in temperature variation that could be expected through improvements in cooling-air pressure drop, power, and fuel-air-ratio distribution were determined. The tests covered a wide range of engine conditions from 500 to 1700 brake horsepower at various values of the over-all fuel-air ratio and cooling-air pressure drop. Distributions of the temperature, the fuel-air ratio, and the cooling-air pressure drop were determined for each test; separate tests were conducted to determine the distribution of engine power.

SYMBOLS

The following symbols are used in this report:

| | |
|------------|---|
| c_p | specific heat of air at constant pressure and normal air temperature, 0.24 Btu per pound per $^{\circ}\text{F}$ |
| g | gravitational acceleration equivalent, 32.2 feet per second per second |
| I | indicated horsepower |
| J | mechanical equivalent of heat, 778 foot-pounds per Btu |
| K | empirical constant of proportionality |
| N | engine speed, rpm |
| n, m | empirical exponents |
| Δp | cooling-air pressure drop, inches of water |
| T_a | cooling-air temperature at cowling entrance, $^{\circ}\text{F}$ |
| T_b | cylinder-barrel temperature, $^{\circ}\text{F}$ |
| T_c | carburetor-deck temperature, $^{\circ}\text{F}$ |
| T_g | mean effective combustion-gas temperature, $^{\circ}\text{F}$ |

- T_{go} mean effective combustion-gas temperature for 0° F manifold-air temperature, $^{\circ}$ F
- T_h cylinder-head temperature, $^{\circ}$ F
- T_m dry manifold-air temperature, $^{\circ}$ F
- U_t supercharger impeller tip speed, feet per second
- σ ratio of cooling-air density to density of Army summer air, 29.92 inches of mercury and 100° F

DESCRIPTION OF TEST EQUIPMENT

Apparatus

The cooling investigation was made with the engine installed in a low-inlet-velocity cowl and mounted on a test stand (fig. 1). This 13-cylinder, double-row, radial, air-cooled engine has a take-off rating of 1850 brake horsepower at an engine speed of 2600 rpm. The engine was equipped with a torquemeter incorporating a 16:9 reduction-gear ratio. The gear-driven single-stage supercharger has low and high gear ratios of 7.6:1 and 9.45:1, respectively. The engine power was absorbed by a $13\frac{1}{2}$ -foot-diameter, three-bladed propeller, operating in a bellmouth installed to prevent backflow around the propeller tips.

The fuel-metering orifice of the injection carburetor used was enlarged to permit extending the investigation to very rich mixtures. The fuel was injected into the combustion-air stream by means of the standard spray ring located at the impeller inlet and rotating with the impeller.

The combustion air was ducted through the intake passages of the cowl. Cooling air was supplied to the engine through a duct, which had a 30-inch-diameter outlet and discharged 4 feet from the cowl entrance. A nearly uniform pressure distribution was attained over the face of the engine by adjusting the position of the duct outlet with respect to the cowl entrance. With this method of supply, values of cooling-air pressure drops up to 15 inches of water were available.

Instrumentation

Pressure tubes. - The pressure of the cooling air upstream of the engine was measured 3 inches ahead of each front-row cylinder by a pair of shielded total-pressure tubes. One tube of each pair was located in front of a cylinder head and the other in front of a cylinder barrel (fig. 2). A vertical rake at the baffle outlet of each cylinder supported two static-pressure tubes behind the head and one static-pressure tube behind the barrel. The tube openings were about 2 inches downstream of the cylinder. Pressures were recorded by photographing a multitube manometer.

Thermocouples. - Temperatures were measured at the rear spark-plug gasket, at a point directly below the rear spark-plug boss, and at the rear middle of the cylinder barrel (fig. 3). The temperature of each rear spark-plug gasket was measured by a gasket-type thermocouple and the temperatures below the spark-plug boss and at the rear middle barrel were obtained by iron-constantan thermocouples embedded approximately one-eighth inch below the surface of the metal.

The temperature of the air entering the cowl was measured by three thermocouples 120° apart and $6\frac{1}{2}$ inches ahead of the front-row cylinders. Thermocouples located on the vertical rakes downstream of each cylinder measured the temperature of the air leaving the head and the barrel of each cylinder. All temperature readings were taken by automatic recording potentiometers.

Exhaust-gas sampling system. - The fuel-air ratios of the individual cylinders were determined from an Orsat analysis of the exhaust gas from each cylinder. Samples of the exhaust gas were obtained through stainless-steel tubes of 1/4-inch diameter located in the stacks immediately downstream of the exhaust port. The intake end of each tube was flattened to form a slot 0.01 inch wide of the type recommended in reference 2 to reduce contamination. A detailed discussion of the sampling equipment and technique used during the tests reported herein is given in reference 3.

Tests were conducted (reference 4) to determine whether the sample obtained from an individual stack was characteristic of that particular cylinder when the engine is equipped with a collector ring. The results of tests made at various engine powers and speeds showed the maximum dilution of the sample to be less than 5 percent, which produced an error of less than 0.001 in the fuel-air ratio.

Cylinder-ignition shorting system. - As a means of determining the distribution of indicated horsepower among the cylinders of the engine, a cylinder-ignition shorting system was installed by which the ignition of any cylinder could be terminated for any desired length of time. When a particular cylinder ceased firing, the total brake horsepower of the engine was reduced by an amount approximating that of the indicated horsepower of that cylinder. The total power of the engine was checked after each cylinder was permitted to fire again to make sure that no change had occurred in engine operating conditions. The ignition of each cylinder was shorted by breaking the high-tension circuit of both spark plugs and grounding the distributor ends of the breaks. As a means of breaking the circuit, the regular ignition leads were removed and auxiliary high-tension wires, which were tapped into the distributor, were led to one of two grounding boxes and then to the cylinder. Remotely controlled solenoids served to break the circuits. No increase in spark-plug gap was necessary to preclude firing in the shorted cylinder. The increase of capacitance resulting from the extension of the high-tension leads did not produce noticeable effects on the spark timing inasmuch as the over-all engine power was not noticeably affected.

METHOD OF TESTS AND CALCULATIONS

Test Procedure

With the exception of tests made to extend the investigation of mixture and power distribution, the procedure of testing was governed by the method to be used in evaluating the cooling data. The relation used in correlating the cooling data, which consists in principle of a balance between the internal and external heat-transfer processes, may be expressed for the cylinder head by

$$\frac{T_h - T_a}{T_g - T_h} = K \frac{I^n}{(\Delta p)^m} \quad (1)$$

A similar equation may be written for the cylinder barrel.

In order to determine the exponents m and n , the cooling-air pressure drop and the engine power, respectively, were independently varied and other conditions were held constant. These tests also allowed calculation of the constant of proportionality K . From tests at various over-all fuel-air ratios, the variation of mean effective combustion-gas temperature with fuel-air ratio was calculated through use of equation (1) in the manner described in reference 1. The test conditions are summarized in the following table:

| Engine power (bhp) | Engine speed (rpm) | Over-all fuel-air ratio | Cooling-air pressure drop (in. water) |
|-----------------------|-----------------------|-------------------------------|---|
| 1000 | 2200 | 0.089 | Varied |
| 1400 | 2400 | .090 | Do. |
| Varied | 2600 | ---do--- | 9.8 |
| Do----- | 2200 | Varied | 8.4 |
| Do----- | 2200 | ---do--- | 7.2 |
| 1000 | 2200 | ---do--- | 9.2 |
| 800 | 2200 | ---do--- | 9.0 |

The cooling tests were confined to engine operation with low supercharger-gear ratio. Tests concerning one variable were usually repeated for several values of the other variables in order to insure generality of the results. At each of the test conditions, complete temperature and pressure data were obtained and exhaust-gas samples were taken.

Because the measurements of individual indicated horsepower values were very time-consuming, this work was done as a separate group of tests in which the engine power was varied from 500 to 1700 brake horsepower and the engine speed ranged from 1600 to 2600 rpm.

Correlation Calculations

Cylinder and cooling-air temperatures and pressures. - The temperatures indicated by the thermocouples located directly below the rear spark-plug boss and at the middle rear barrel were used in evaluating the constants of equation (1) for the head and the barrel, respectively, and will hereinafter be denoted head temperature and barrel temperature. The average head and barrel temperatures for the 18 cylinders were used in evaluating the over-all head and barrel relations. For convenience, the cooling-air temperature T_a was considered to be the temperature of the air entering the cowling.

The cooling-air pressure drop used for the cooling calculations of each cylinder was measured as the difference between the total pressures upstream from the cylinders (fig. 2) and the static pressures behind the head and the barrel of each cylinder. The cooling-air pressure drop for the correlation of over-all cooling data was taken as the average of these individual pressure drops. The value of σ was calculated as the ratio of the mean of upstream and downstream air densities to the sea-level air density for Army summer air. The

upstream air density was based on upstream total pressure and cooling-air temperature; the downstream air density was based on the temperature and pressure measured by the rakes.

Mean effective combustion-gas temperature. - By the use of the method described in reference 1, the variation of the mean effective combustion-gas temperature was calculated by use of equation (1) from the tests during which only the fuel-air ratio was varied. The effective gas temperature was assumed to vary with the manifold temperature.

$$T_g = T_{go} + 0.80 T_m \quad (2)$$

Owing to the presence of vaporized fuel, accurate determination of the manifold temperature T_m is difficult. Consequently, the dry manifold temperature is usually calculated from the carburetor-deck temperature and the theoretical temperature rise through the supercharger as

$$T_m = T_c + \frac{U_t^2}{c_p g J} \quad (3)$$

For low supercharger-gear ratio, this equation may be numerically evaluated as

$$T_m - T_c = 22.1 \left(\frac{N}{1000} \right)^2 \quad (4)$$

Indicated horsepower. - Because the charge-air weight for each cylinder is a very difficult quantity to measure, the correlation calculations for the entire engine and for the individual cylinders were based on values of total indicated horsepower and the indicated horsepower of the individual cylinders, respectively. Through the use of unpublished data for the total friction horsepower at full-open throttle (fig. 4), which also have indicated that the throttle position and the manifold pressure have little effect upon the total friction horsepower, the total indicated horsepower was taken as the sum of the total brake horsepower and the total friction horsepower. Distribution patterns of the indicated horsepower for different periods of the test program at comparable engine conditions are shown in figure 5. From this figure it can be seen that the indicated-horsepower distribution is not perfectly reproducible but the maximum variation is only 4.4 percent. The indicated-horsepower distribution was determined by averaging a number of such test runs. Because of possible inaccuracies in the friction-horsepower curve or a consistent error in the use of the cylinder-ignition shorting system, the sum of the individual indicated horsepower did not equal the actual total indicated horsepower; however, the variation was usually within ± 5 percent. In order to be consistent in calculations,

the measured values of individual indicated horsepower were inversely varied as the ratio of their sum to the actual total indicated horsepower.

RESULTS AND DISCUSSION

Engine-Cooling Characteristics

The results of correlating the average cooling data are shown in figure 6 for the cylinder heads and the cylinder barrels. The constants of equation (1) are defined by the curves of figure 6 and the relations among the cooling variables may be expressed as

$$\frac{T_h - T_a}{T_g - T_h} = 0.00566 \frac{I^{0.69}}{(\Delta p)^{0.35}} \quad (\text{Head}) \quad (5)$$

$$\frac{T_b - T_a}{T_g - T_b} = 0.0137 \frac{I^{0.62}}{(\Delta p)^{0.45}} \quad (\text{Barrel}) \quad (6)$$

The experimentally determined variation of mean effective combustion-gas temperature with over-all fuel-air ratio is shown for cylinder heads and cylinder barrels in figure 7 for a manifold temperature of 0° F.

In order to facilitate the determination of a trend that can be effected by the variation of one of the engine operating conditions, the cooling relation for the cylinder heads (equation (5)) may be slightly modified as

$$\frac{T_h - T_a}{T_g - T_a} = \frac{1}{1 + \frac{(\Delta p)^{0.35}}{0.00566 I^{0.69}}} \quad (7)$$

and presented in graphical form. The effects of fuel-air ratio, carburetor-deck temperature, and engine speed are incorporated in the complete graphical solution of equation (7) as shown in figure 8. The relations between the various component curves as well as the general procedure for applying the composite curve is indicated on the graph and an illustrative example is presented in the appendix. Problems involving the manipulation of equation (5) may be quickly solved through use of figure 8. Because the graphical analysis not only takes into account cooling equation (7) but also the effects of fuel-air ratio, carburetor-deck temperature, and

engine speed, it offers a convenient method of quickly observing the effects of variations in the average engine data for this particular installation.

The relation between the average cylinder-head temperature and the average rear spark-plug gasket (fig. 9) enables over-all cooling computations to be based on the rear-spark-plug-gasket temperature as well as on the cylinder-head temperature.

Cylinder-Temperature Distribution

The observed temperatures of the individual cylinder heads and cylinder barrels are presented in figures 10 and 11, respectively, together with the corresponding values of cooling-air pressure drop, indicated horsepower, and fuel-air ratio for four values of engine power. The dashed line through each temperature pattern indicates the average cylinder temperature computed from the over-all correlation expression (equations (5) and (6)). The striking feature exhibited by the temperature patterns is the tendency of the front-row cylinders to operate considerably hotter (in some cases as much as 125° F for the cylinder heads) than the rear-row cylinders. Figures 10 and 11 also show systematic variations in indicated horsepower and cooling-air pressure drop between the front- and the rear-row cylinders.

Effect of cooling-air pressure drop distribution. - From preliminary tests, little variation in cooling-air pressure upstream from the cylinder was observed between front- and rear-row cylinders. Consequently, the larger part of the pressure-drop variation results from differences between the pressures at the cylinder outlet for the two rows. Because the passage between the front-row baffle outlet and the adjacent two rear-row cylinders appears to be the source of considerable mixing loss in addition to that occurring downstream from the engine, the pressure drop across the rear-row cylinders will be greater than that across the front-row cylinders. Differences in the cooling-air flow characteristics and in the pressure losses may be expected in the test stand and in flight owing to the difference between the methods of supplying cooling air. Although the weight of cooling-air flow is important as far as heat transfer is concerned, the pressure drop may be used as an indication of the weight flow inasmuch as unpublished calibration tests conducted at Cleveland indicate that the pressure-drop weight-flow relations were the same for the cylinders of either row.

Effect of power distribution. - The indicated-horsepower values of the front-row cylinders are generally greater (fig. 10) than those of the rear-row cylinders; approximately 51.3 percent of the

total power was developed by the front-row cylinders and 48.7 percent by the rear-row cylinders. This situation may be partly explained by the fact that the intake pipes leading to the front-row cylinders are considerably longer than those leading to the rear-row cylinders. The longer intake pipes provide additional inertia supercharging for the front-row cylinders, and, consequently, these cylinders develop noticeably greater powers and higher cylinder temperatures than do the rear-row cylinders. A power variation of the size observed, however, contributes the smaller portion of the temperature difference between the two rows.

Effect of fuel-air-ratio distribution. - Because no systematic differences were observed between the fuel-air-ratio patterns of the two cylinder rows (fig. 10), the difference in the temperature levels of the two cylinder rows will not depend upon the fuel-air-ratio pattern. It appears that the circumferential distribution of temperature may be considerably influenced by variation in fuel-air ratio. In order to substantiate the fact that cylinder-head temperature distribution is sensitive to the fuel-air-ratio variations, figure 12 is presented showing tests in which the mixture distribution was changed by varying the throttle angle while other engine conditions were held constant. The procedure used for these tests is explained in reference 3. The fuel-air-ratio distributions are given for 1000 brake horsepower at full-open throttle and at the throttle angle required to develop that power with sea-level carburetor-deck pressure. The changes in the cylinder-head temperature distribution (fig. 12) resulted directly from the corresponding changes in fuel-air-ratio distribution.

Correlation of Individual Cylinder Temperatures

In order to observe the relation between the temperature distribution and the distributions of cooling-air pressure drop, engine power, and fuel-air ratio, the cooling data for each of the cylinders were separately correlated. A comparison of the correlated cooling data for each cylinder with the correlated cooling data for the entire engine (equations (5) and (6)) is shown in figure 13. For each cylinder, the exponents m and n of equation (1) were found to be very nearly 0.35 and 0.69, respectively, for the head and 0.45 and 0.62, respectively, for the barrel, the values determined by the over-all cooling data. A study of the results showed the slopes of the correlation curves of the individual cylinders to be in agreement; however, a variation exists in the levels of the correlation curves from which it is evident that factors are present in the relation between the cylinders and cooling variables other than those considered in the cooling correlation. Consequently, even though

there would be perfect distribution of the cooling-air pressure drop, power, and fuel-air ratio, unequal temperature distribution would be encountered. Apart from the experimental error involved, variations in the levels of the individual cylinder correlation curves may result from uncontrollable and unaccountable variables and small variations in instrumentation.

In order to extend the study of the magnitude of temperature variations among cylinders and to investigate the extent to which each cylinder operated as an isolated single cylinder responding to its own set of operating conditions, the temperatures corresponding to the cooling-air pressure drop, power, and fuel-air ratio of each cylinder were calculated (using a modified form of the over-all cooling relations, equations (5) and (6)) and compared with the observed values. These comparisons are shown in figures 14 and 15 for the cylinder heads and cylinder barrels, respectively, at four values of total engine power. Although the computed temperature distributions are very similar to the observed values, discrepancies in temperatures averaging 20° F exist and emphasize the importance of extraneous effects on cylinder temperature. A direct correspondence is apparent, however, between the existing temperature distribution and the distributions of cooling-air pressure drop, power, and fuel-air ratio.

The foregoing results also indicate that a definite limit exists for the improvement in temperature distribution that may be attained by producing uniform distributions of cooling-air pressure drop, power, and fuel-air ratio. The temperature variations remaining after solving the distribution problems appear to be approximately the magnitude of the differences between the actual and the calculated temperatures shown in figures 14 and 15 and will therefore average $\pm 20^{\circ}$ F.

SUMMARY OF RESULTS

The analysis of the cooling data and the study of the distributions of cylinder temperature, cooling-air pressure drop, power, and fuel-air ratio on a double-row radial aircraft engine indicate that:

1. Through use of the cooling equation, the slopes of the individual-cylinder correlation curves were the same, however, a variation existed in the levels of the correlation curves. Consequently, even though there would be perfect distribution of the cooling-air pressure drop, power, and fuel-air ratio, unequal temperature distribution would be encountered.

2. For engine powers from 1000 to 1700 brake horsepower, a direct correspondence existed between the cylinder-temperature patterns and the distributions of cooling-air pressure drop, power, and fuel-air ratio.

3. The observed individual cylinder-head temperatures and the cylinder-head temperatures calculated from the individual cylinder operating conditions differed by an average of 20° F. The temperature variations among cylinders that will remain after improvement in distribution of cooling-air pressure drop, power, and fuel-air ratio will be an average of $\pm 20^{\circ}$ F, the same order as the difference between the actual and computed temperature distribution.

Aircraft Engine Research Laboratory,
National Advisory Committee for Aeronautics,
Cleveland, Ohio.

APPENDIX - USE OF GRAPHICAL COOLING ANALYSIS

The use of the graphical cooling analysis of figure 8 is illustrated by an example in which the cylinder-head temperature is found from the engine operating and cooling condition. The result is compared with that calculated by means of equation (5).

The following engine conditions are assumed:

| | |
|--|-------|
| Over-all fuel-air ratio | 0.092 |
| Engine speed, rpm | 2200 |
| Brake horsepower | 1400 |
| Friction horsepower | 236 |
| Effective pressure drop, in. water | 8.40 |
| Cooling-air temperature, °F | 53 |
| Carburetor-deck temperature, °F | 65 |

In order to find the cylinder-head temperature from figure 8, the following steps must be taken:

1. Find the value of 0.092 for the fuel-air ratio and drop vertically to point 1; move horizontally to point 2 thus accounting for the effects of carburetor-deck temperature and engine speed.

2. Move vertically to point 3 and then horizontally to point 4 to find the line of constant $T_g - T_a$.

3. From a cooling-air pressure drop of 8.40 inches of water, move vertically to the line of constant indicated horsepower of 1636 (point 5) and then horizontally to point 6. A junction is then made with the line of constant $T_g - T_a$ originating from point 4.

4. Move vertically from point 6 to a value of 324° F indicated for $T_h - T_a$. Add the cooling-air temperature of 53° F (point 3) to the value of $T_h - T_a$ to obtain the value of 377° F for the average cylinder-head temperature.

By means of equation (5), the cylinder-head temperature is computed as 380° F.

It is evident that by a method similar to that presented in the preceding example, figure 8 may be used to find the required cooling-air pressure drop, the indicated horsepower, or the fuel-air ratio when all other conditions are known. The figure, however, does not lend itself easily to the determination of cooling-air temperature.

REFERENCES

1. Pinkel, Benjamin: Heat-Transfer Processes in Air-Cooled Engine Cylinders. NACA Rep. No. 612, 1938.
2. Cook, Harvey A., and Olson, Walter T.: Small-Orifice Tubes for Minimizing Dilution in Exhaust-Gas Samples. NACA ARR, Feb. 1943.
3. Marble, Frank E., Butze, Helmut F., and Hickel, Robert O.: Study of the Mixture Distribution of a Double-Row Radial Aircraft Engine. NACA ARR No. E5I05, 1945.
4. Butze, Helmut F.: Dilution of Exhaust-Gas Samples from a Multi-cylinder Engine Equipped with an Exhaust-Gas Collector. NACA RB No. E5B10, 1945.

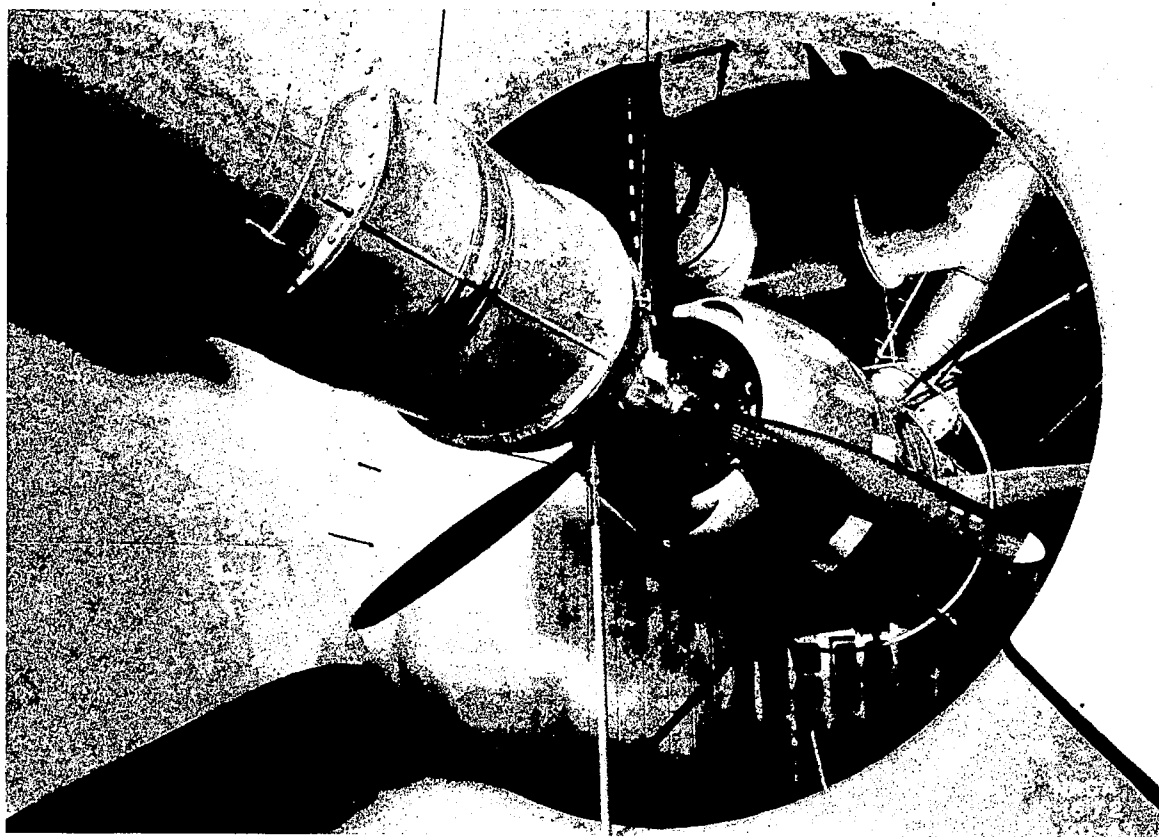


Figure 1. - Installation of test engine.

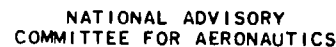


Figure 2. - Side view of cooling-air pressure tube and thermocouple installation with trailing edge of baffles cut away.

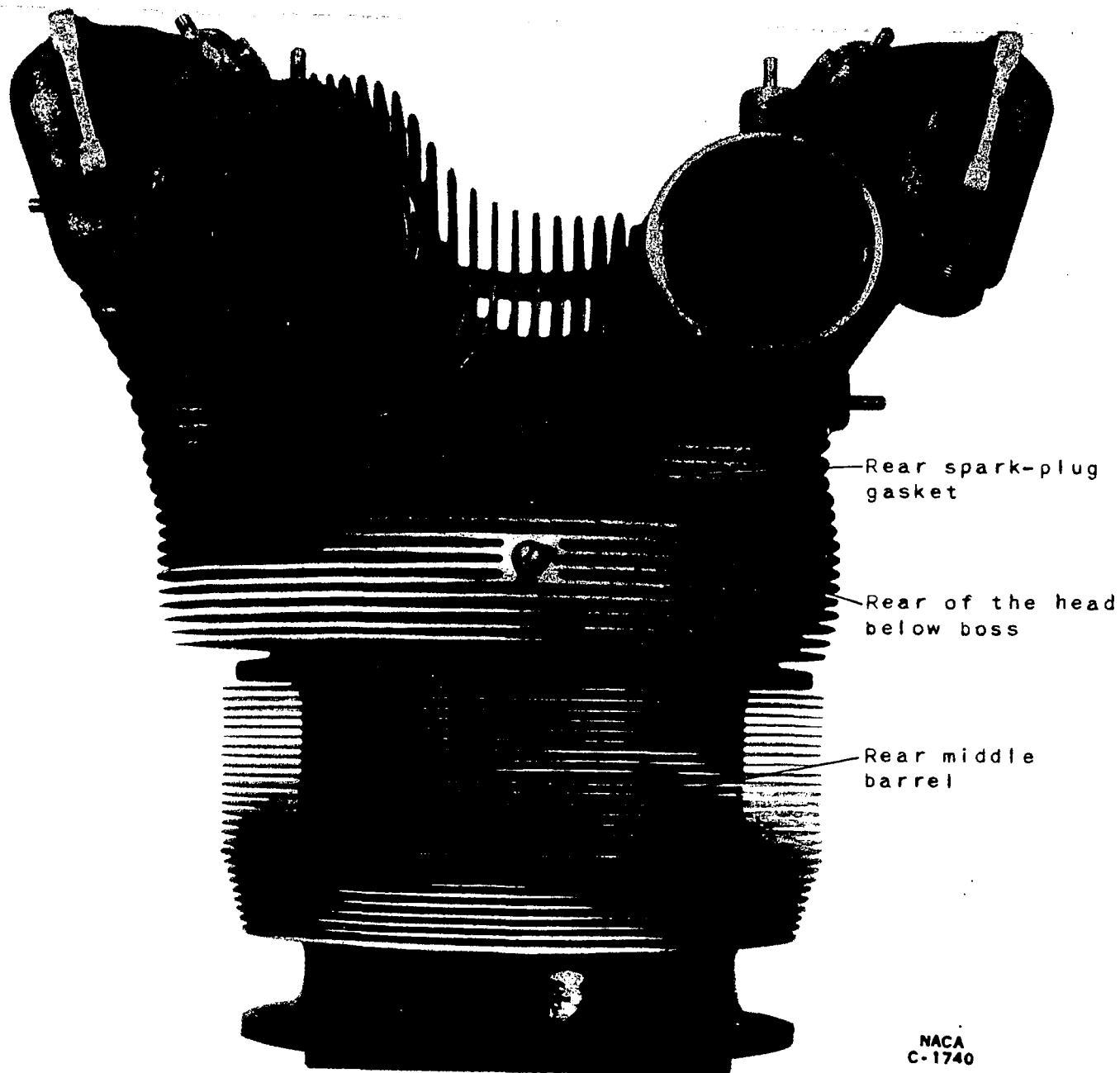


Figure 3. - Location of cylinder thermocouples.

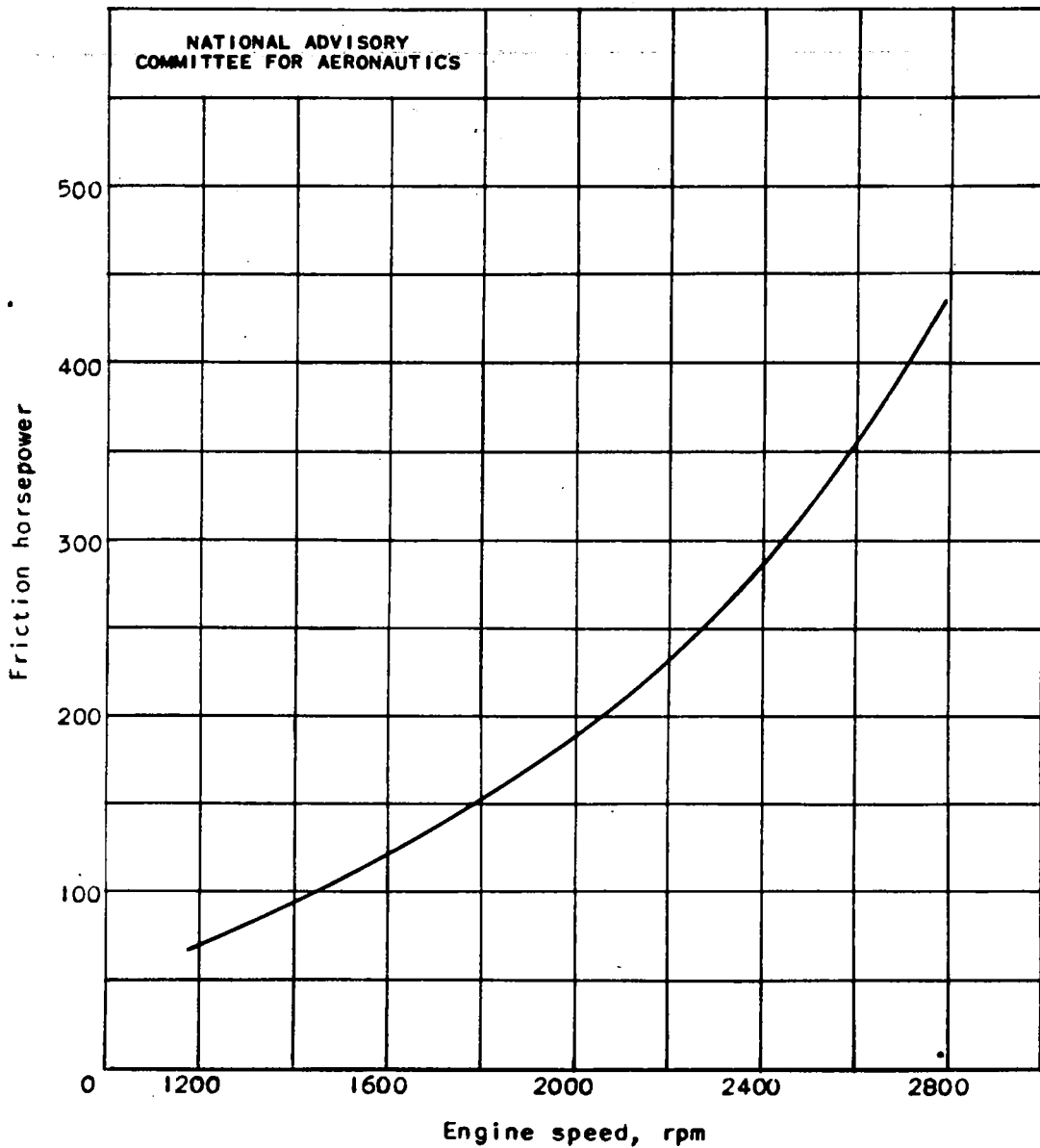


Figure 4. - Values of friction horsepower at various engine speeds with full-open throttle and supercharger in low-gear ratio. (Data from unpublished dynamometer tests.)

Fig. 5

NACA ARR No. E6C01

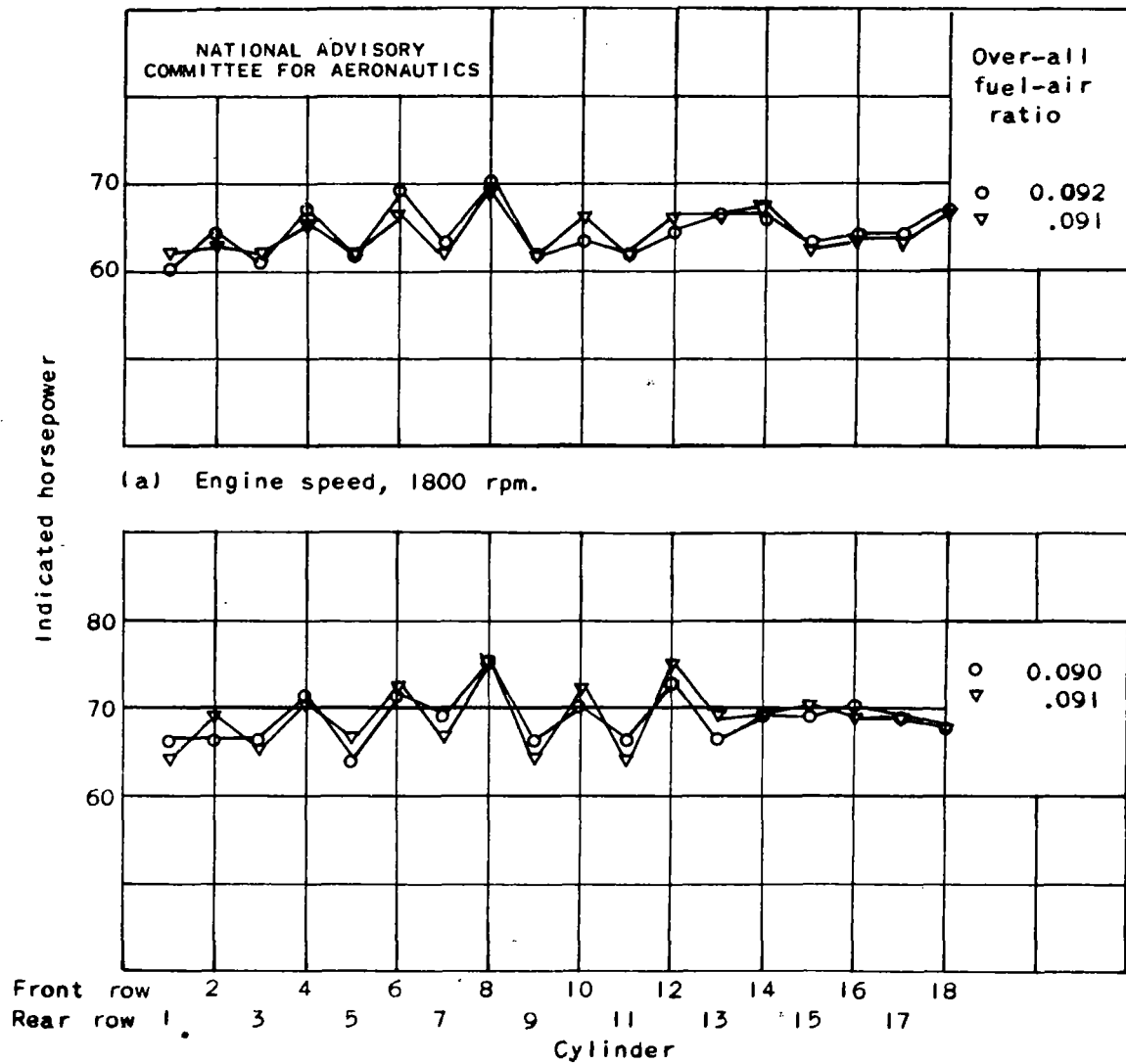


Figure 5. - Reproducibility of indicated horsepower distribution patterns.
Brake horsepower, 1000.

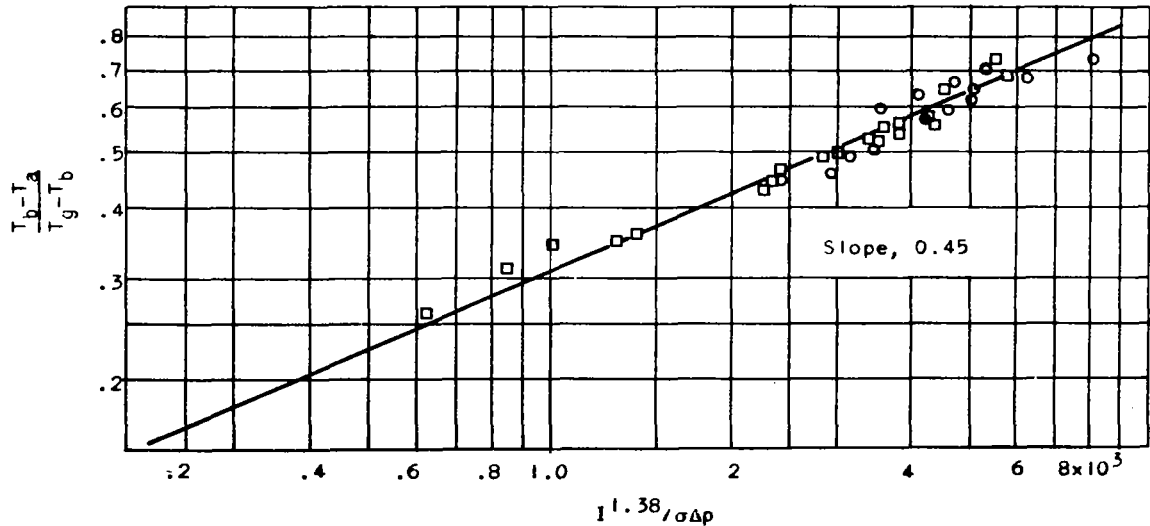
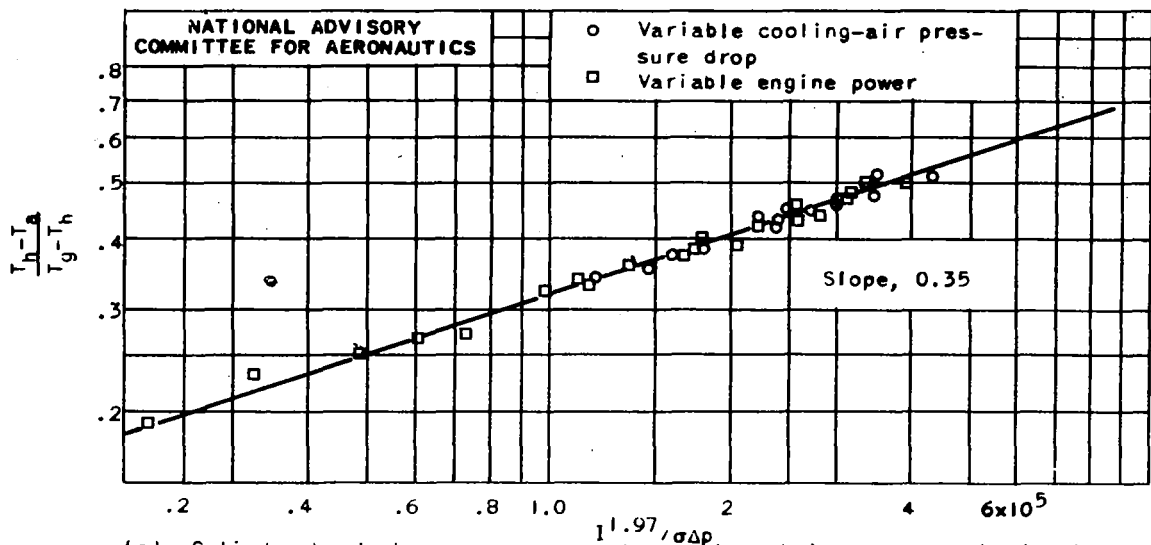


Figure 6. - Correlation of over-all cooling data referred to engine indicated horsepower and cooling-air pressure drop.

Fig. 7

NACA ARR No. E6C01

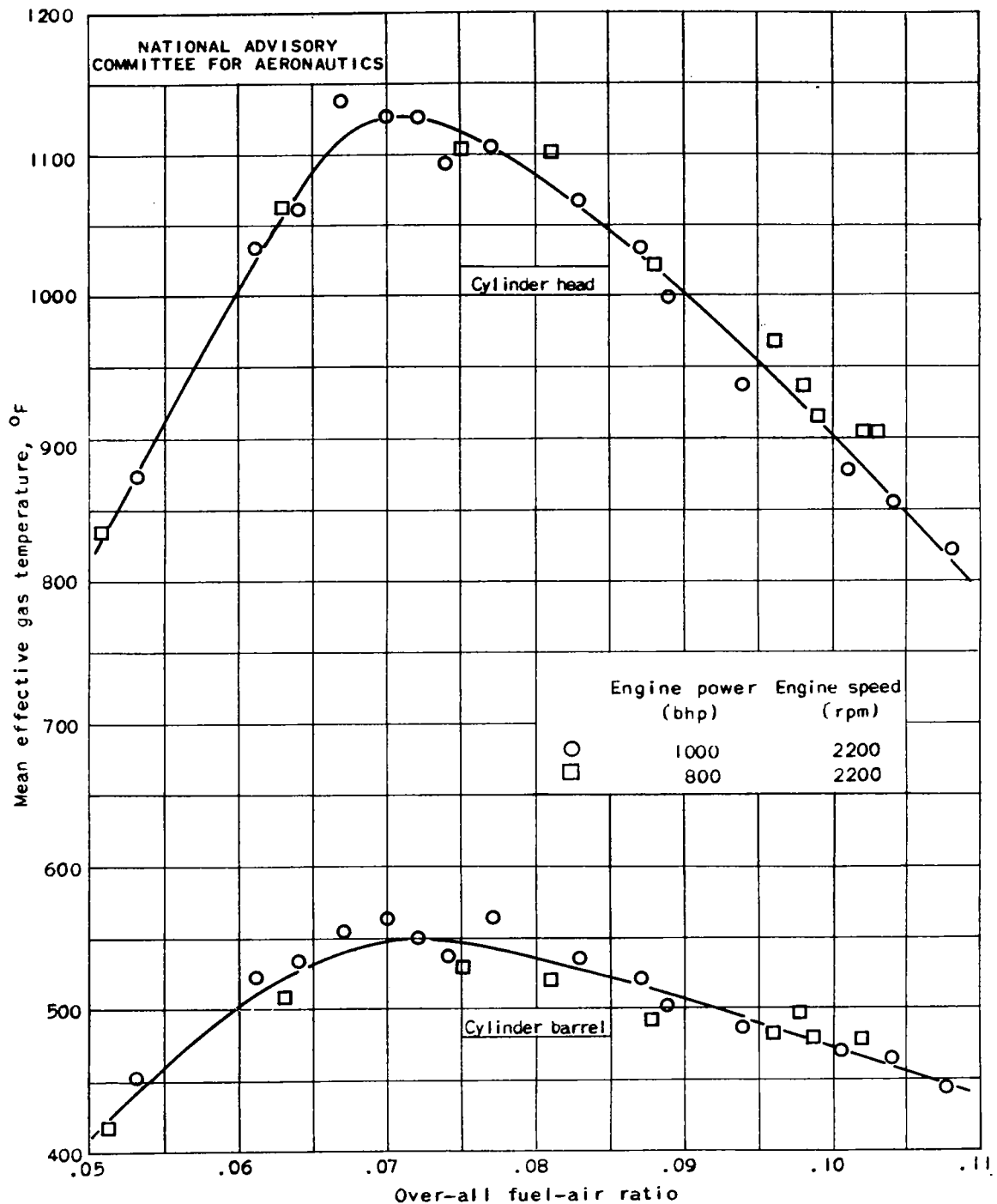


Figure 7. - Variation of mean effective combustion-gas temperature with over-all fuel-air ratio corrected to manifold-air temperature of 0° F.

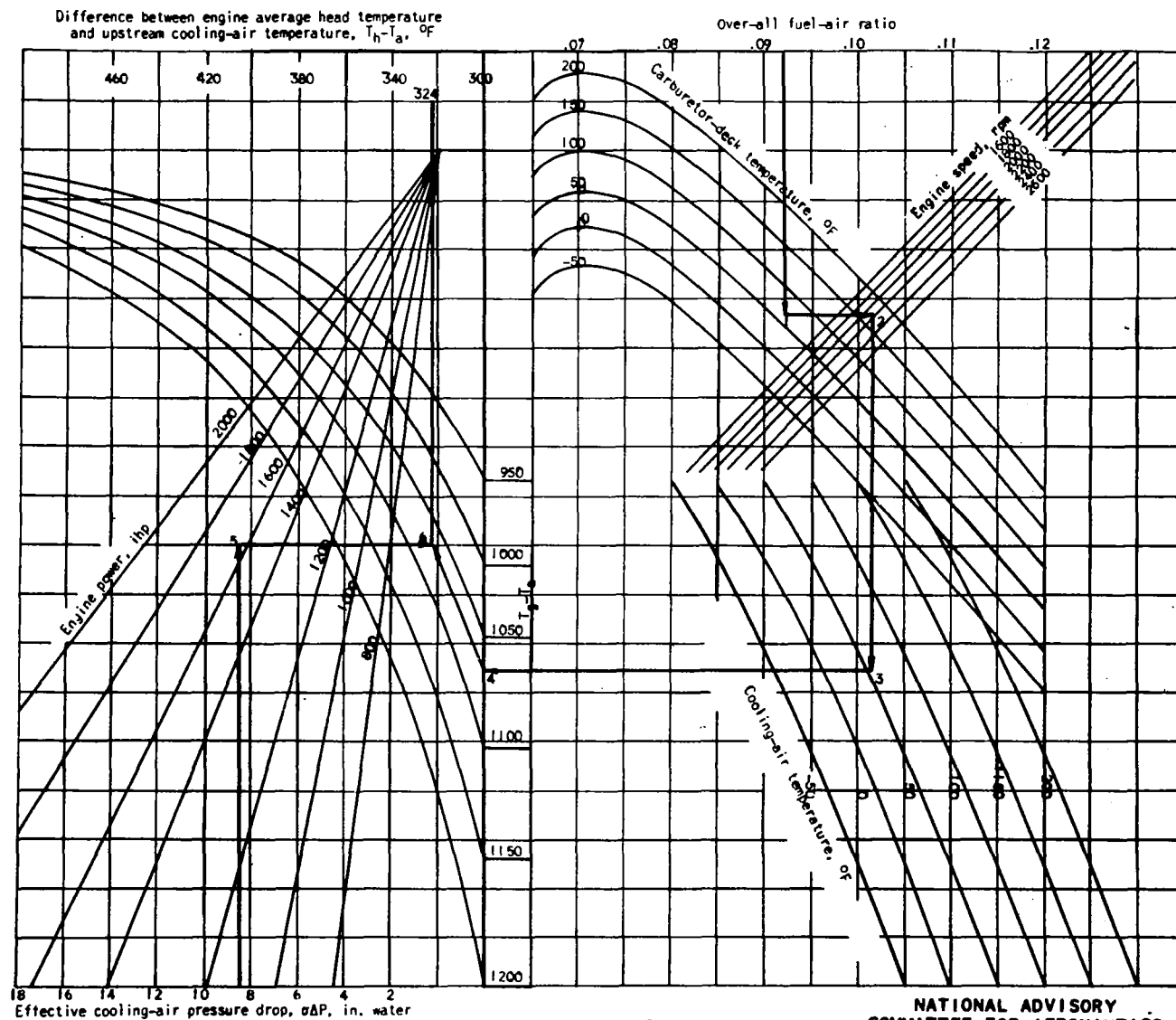


Figure 8. - Graphical presentation of cooling relation for cylinder head of engine operating at low supercharger-gear ratio. Based on average temperature below rear spark-plug bosses.

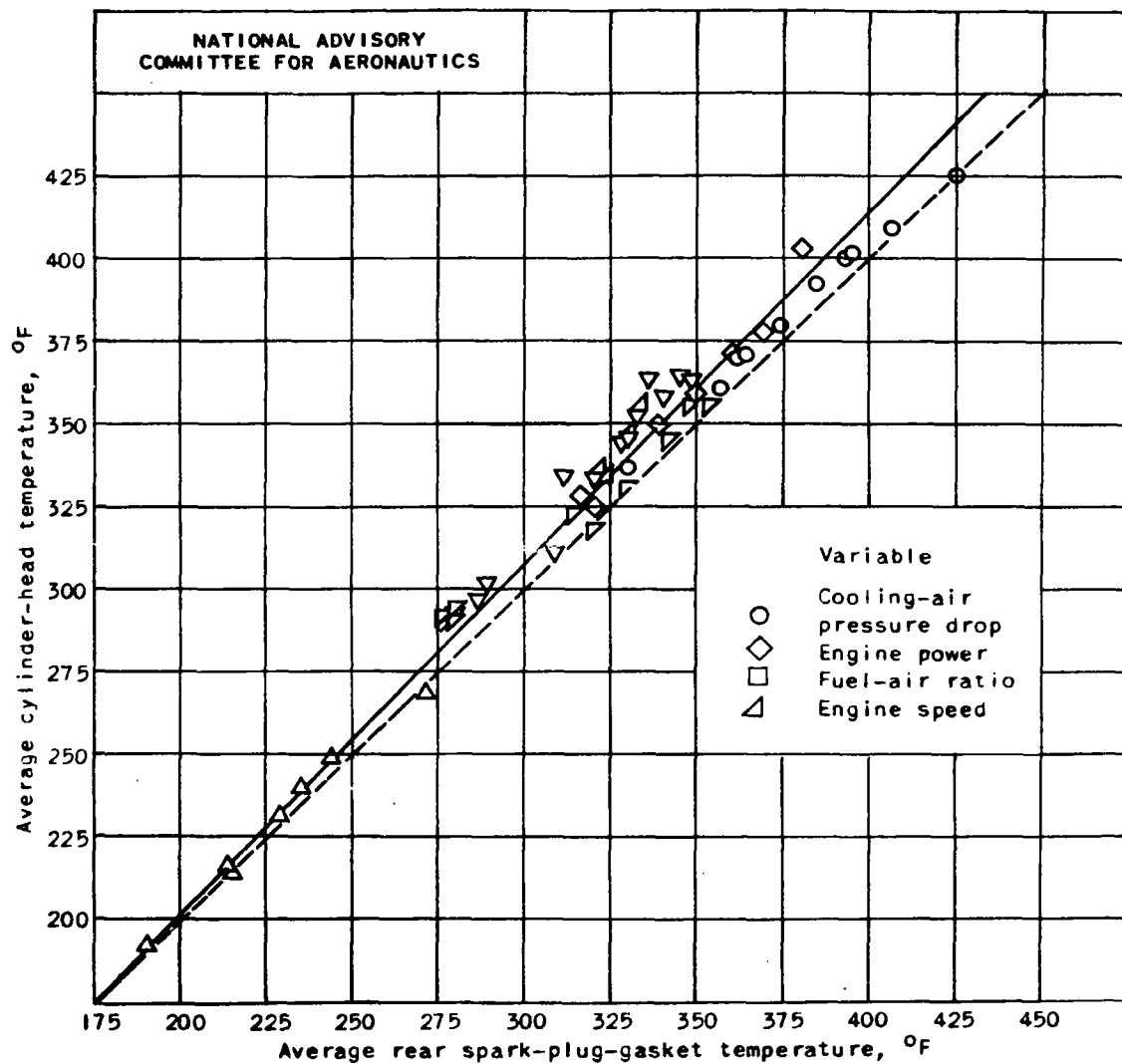


Figure 9. - Relation between average temperature of 18 cylinder-head embedded thermocouples with average temperature of rear spark-plug-gasket thermocouples.

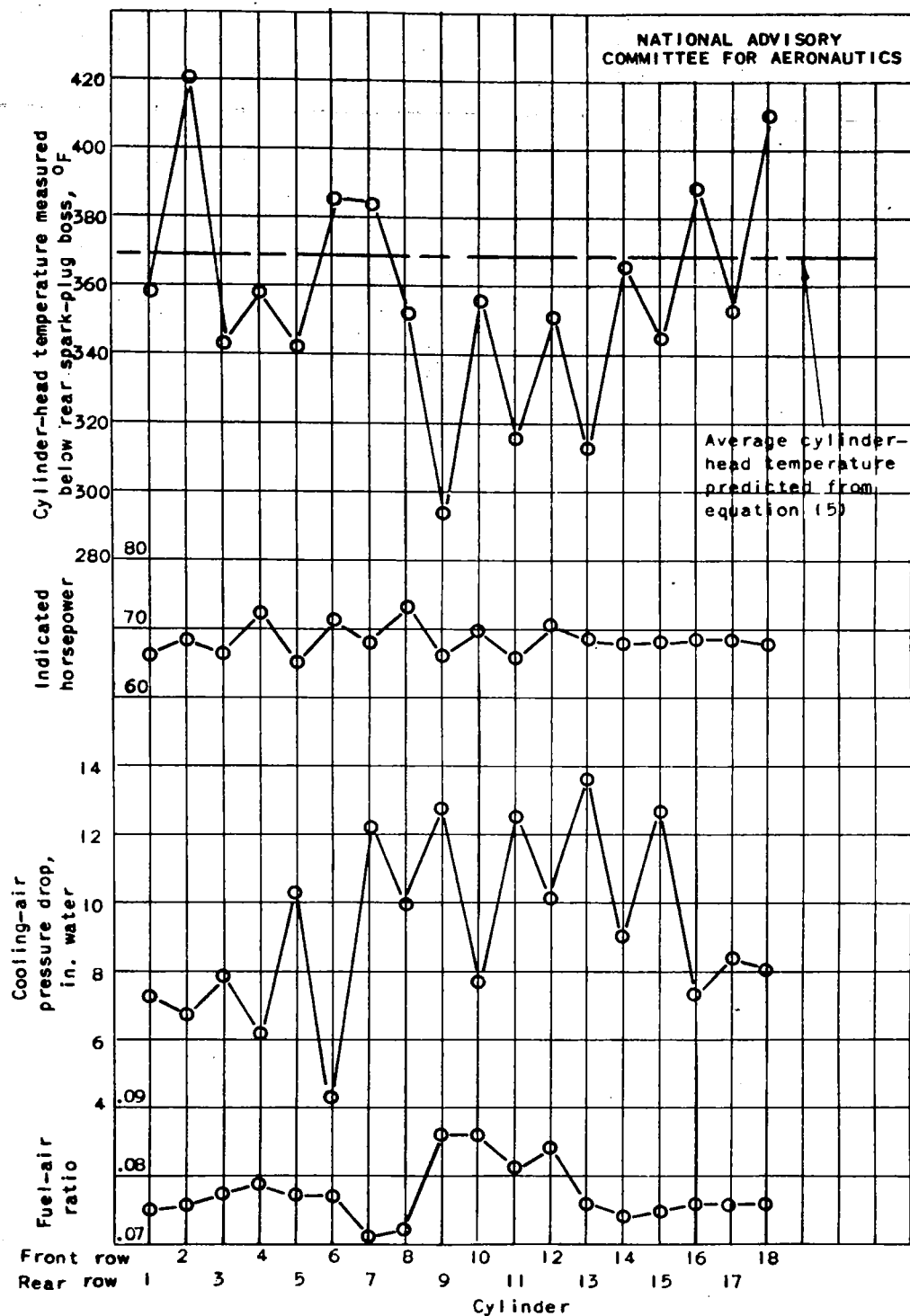
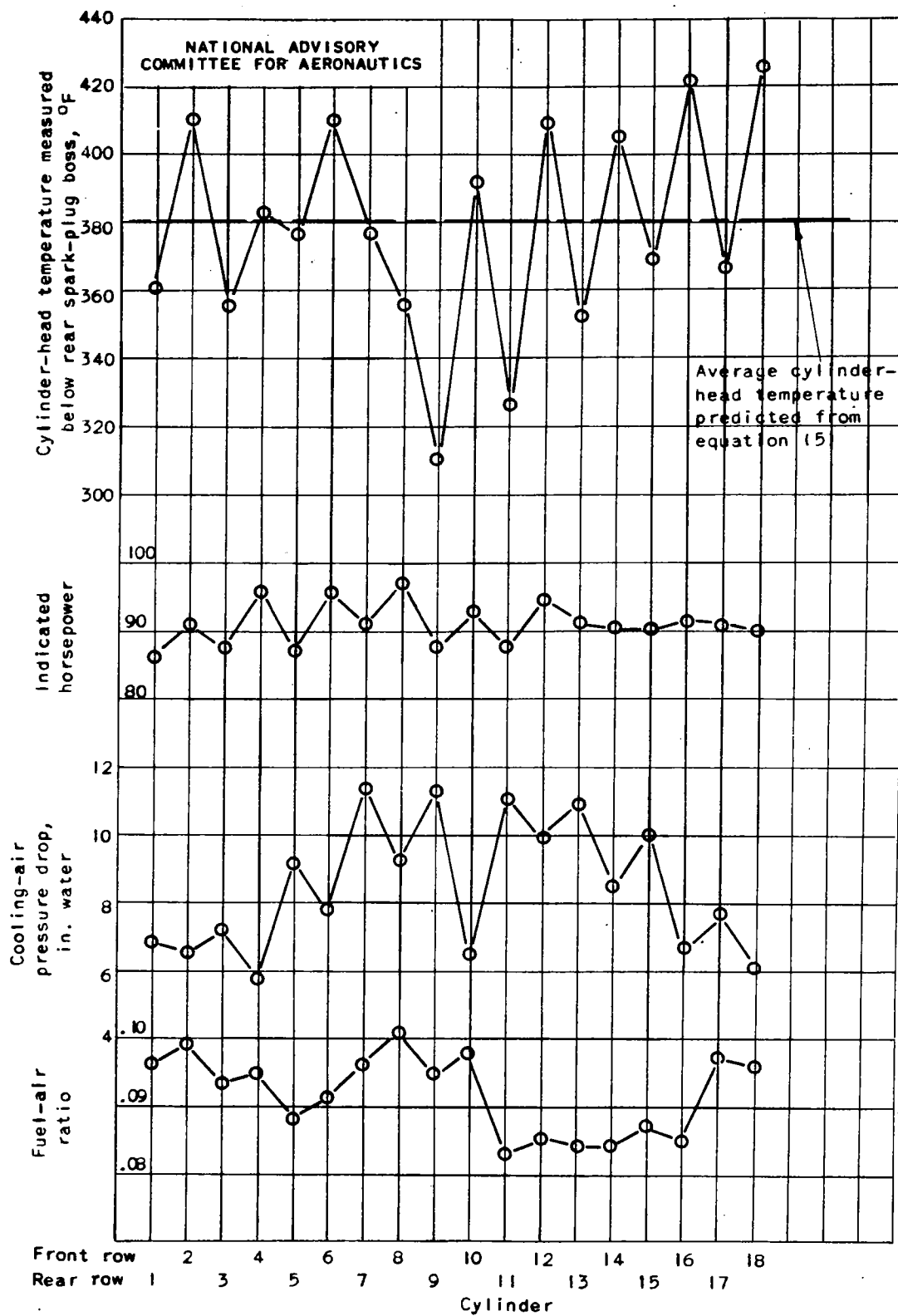


Figure 10. - Distribution of cylinder-head temperature, indicated horsepower, cooling-air pressure drop, and fuel-air ratio among the cylinders. Supercharger in low-gear ratio.

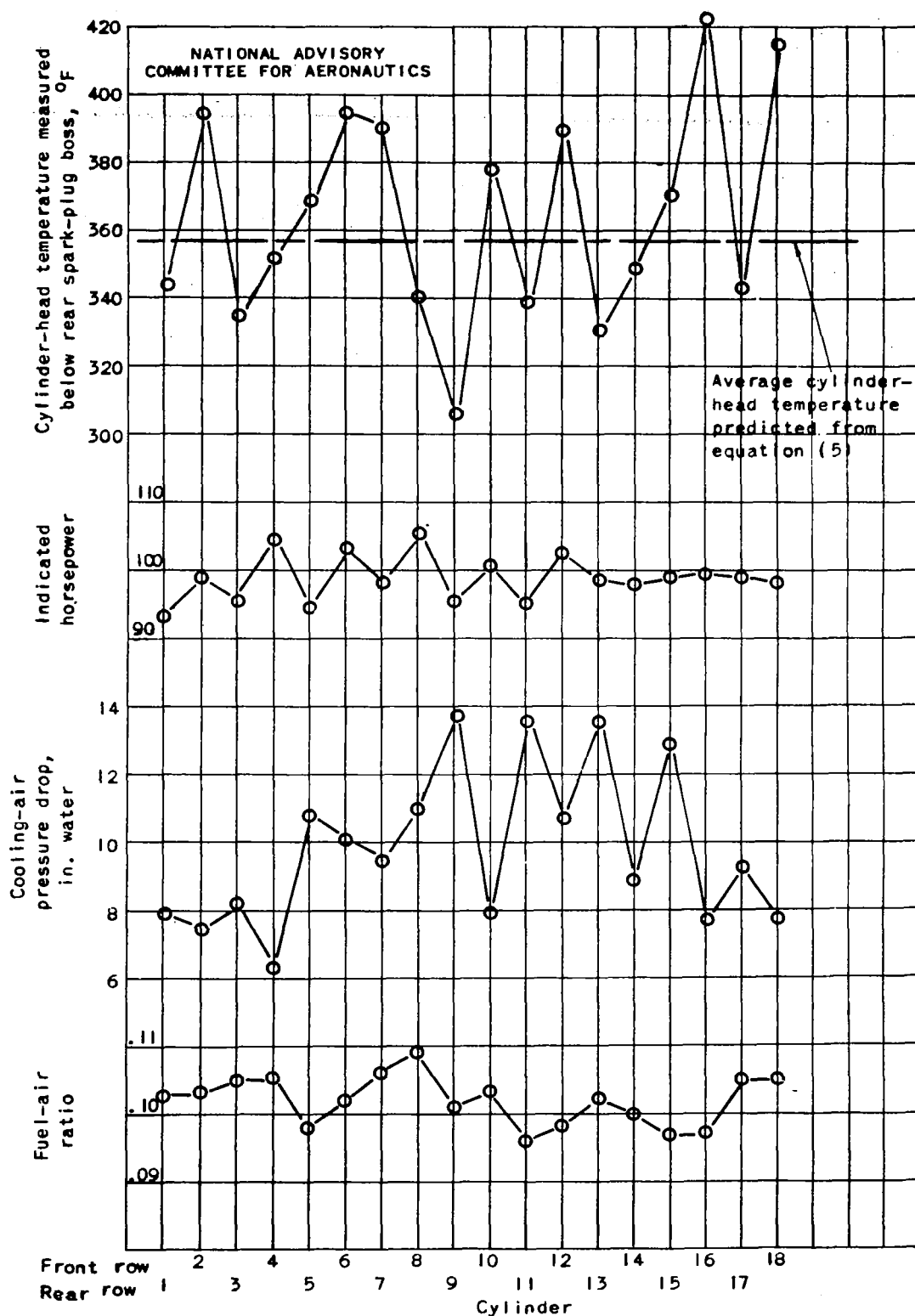
Fig. 10b

NACA ARR No. E6C01



(b) Brake horsepower, 1400; engine speed, 2200 rpm.

Figure 10. - Continued.

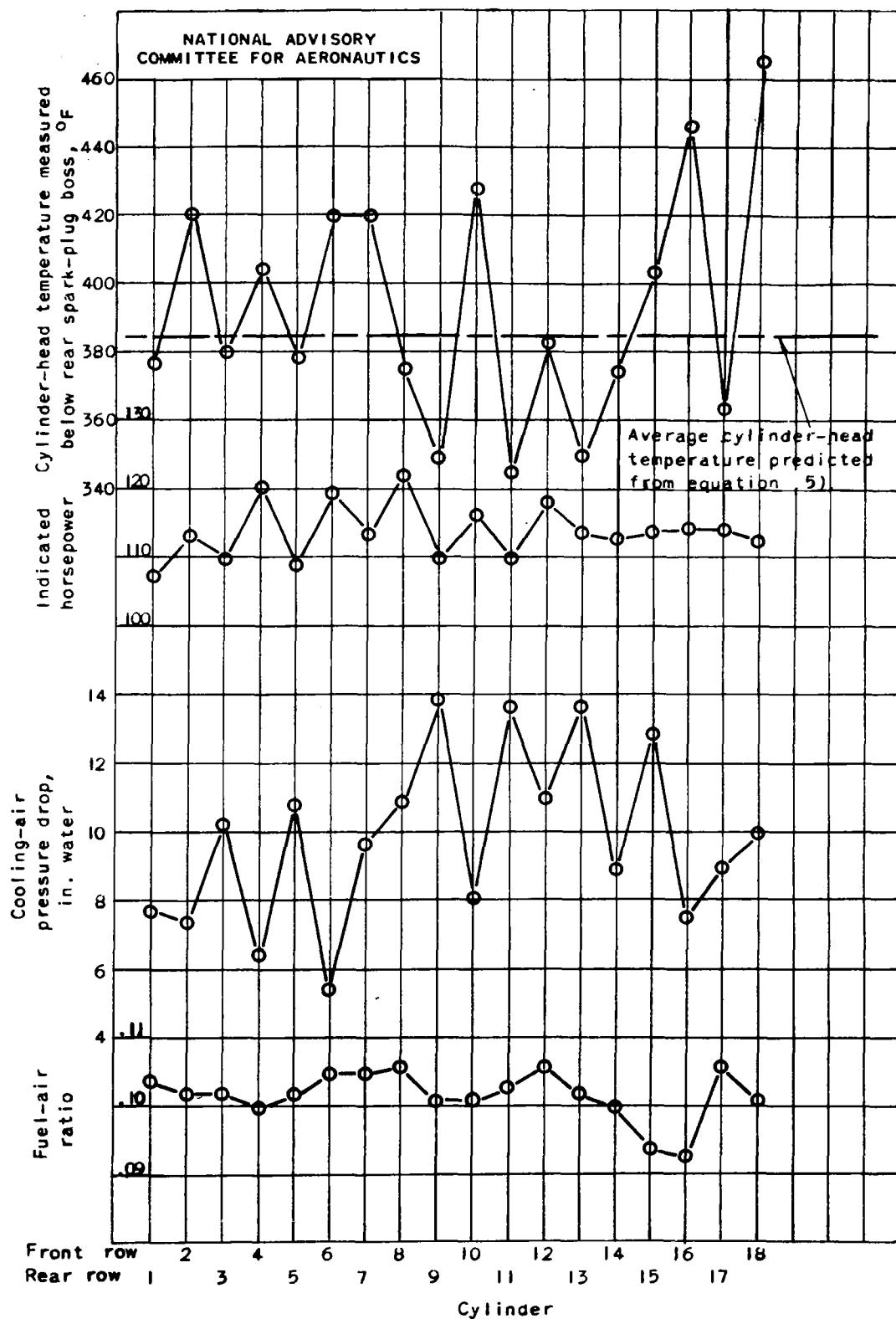


(c) Brake horsepower, 1500; engine speed, 2400 rpm.

Figure 10. - Continued.

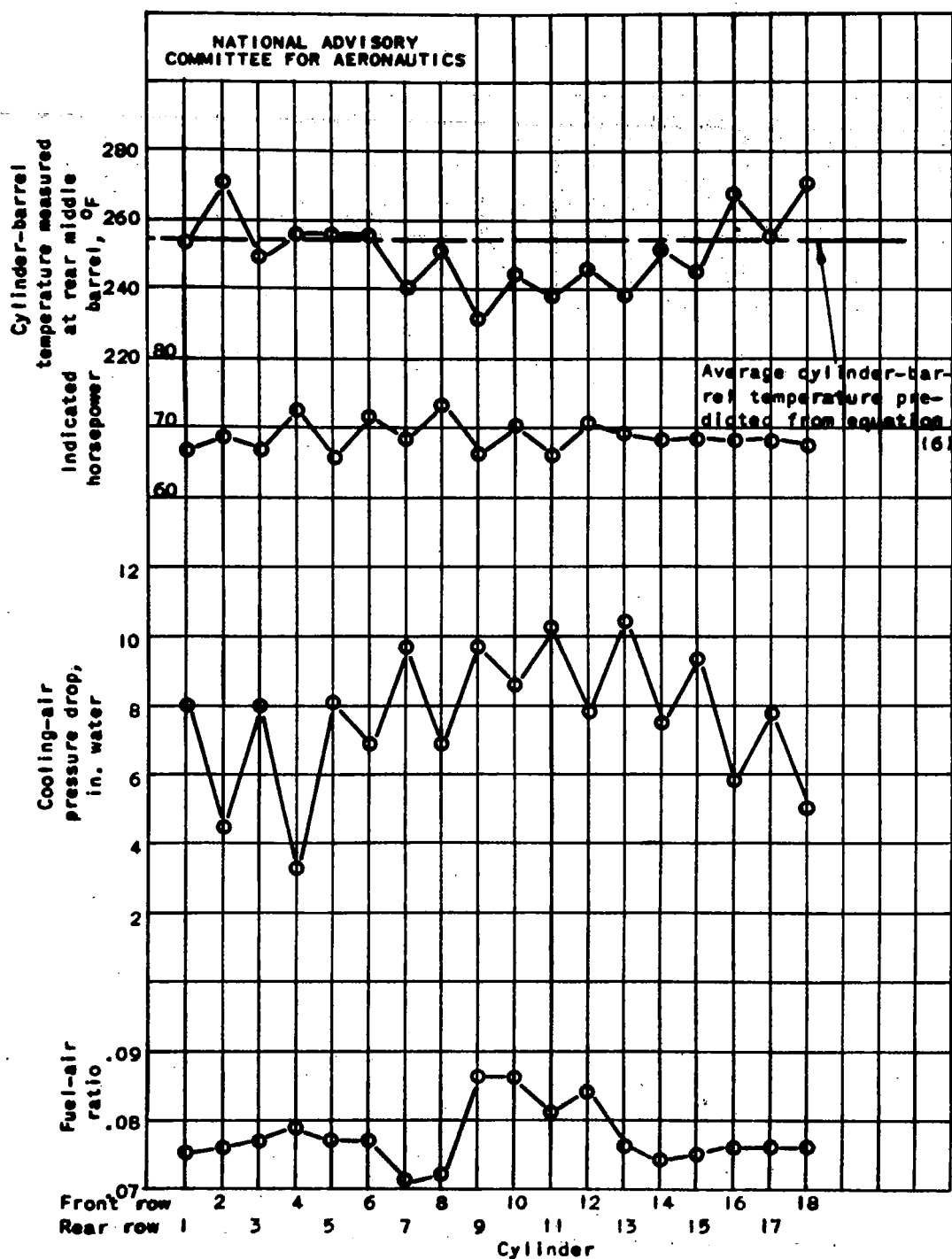
Fig. 10d

NACA ARR No. E6C01



(d) Brake horsepower, 1700; engine speed, 2600 rpm.

Figure 10. - Concluded.

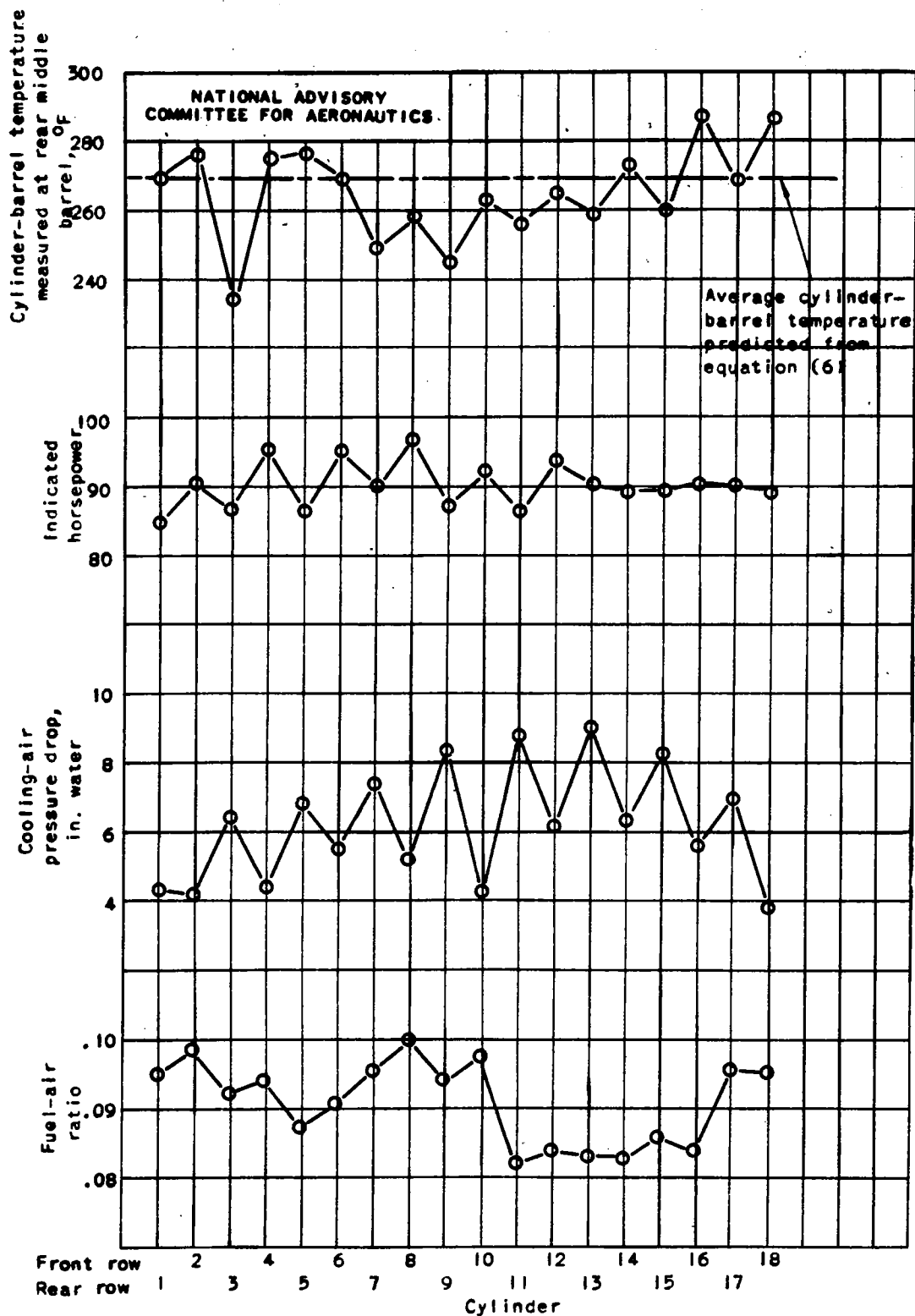


(a) Brake horsepower, 1000; engine speed, 2200 rpm.

Figure 11. - Distribution of cylinder-barrel temperature, indicated horsepower, cooling-air pressure drop, and fuel-air ratio among the cylinders. Supercharger in low-gear ratio. (Dotted lines indicate that data were unavailable on the intervening cylinders.)

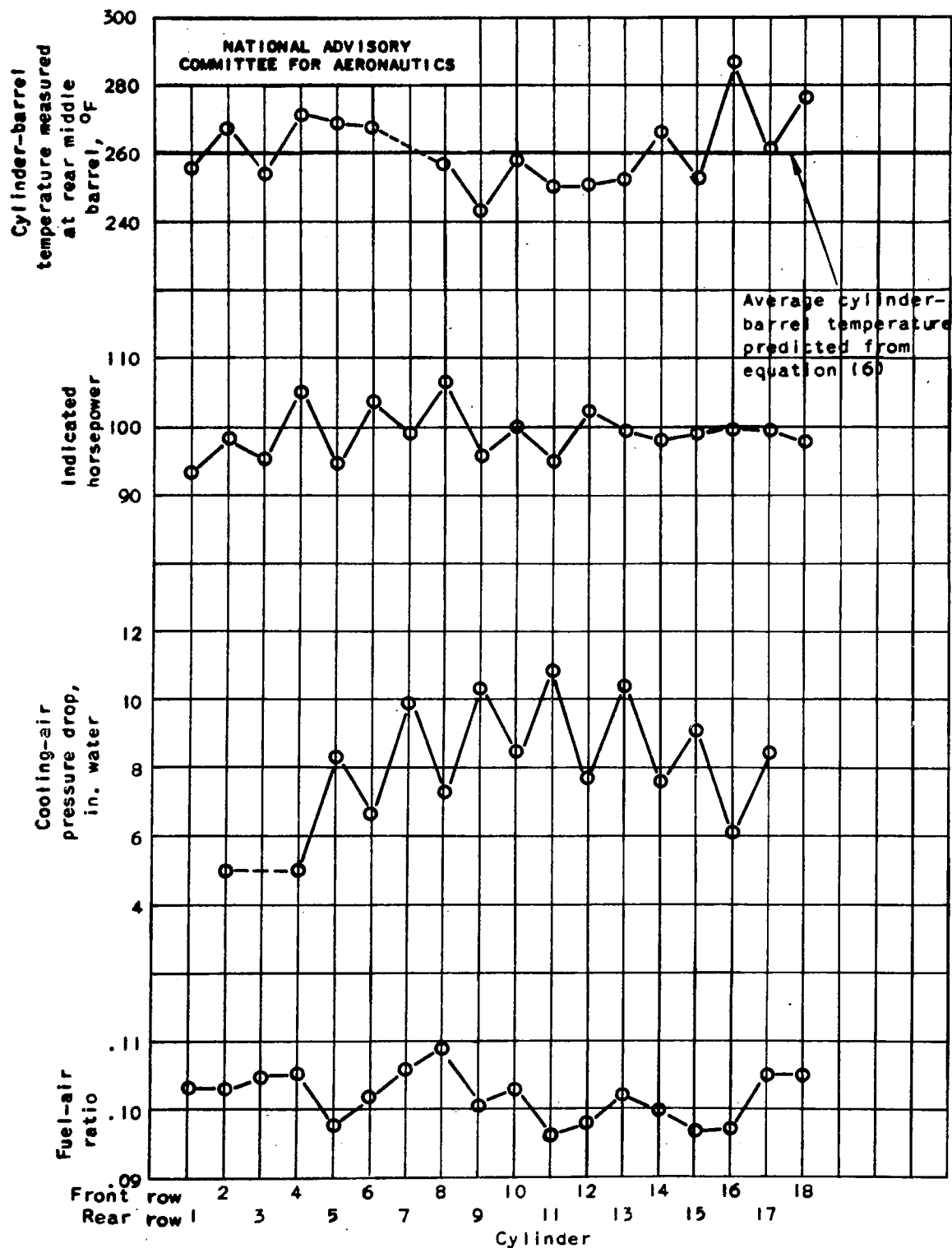
Fig. 11b

NACA ARR No. E6C01



(b) Brake horsepower, 1400; engine speed, 2200 rpm.

Figure 11. - Continued.

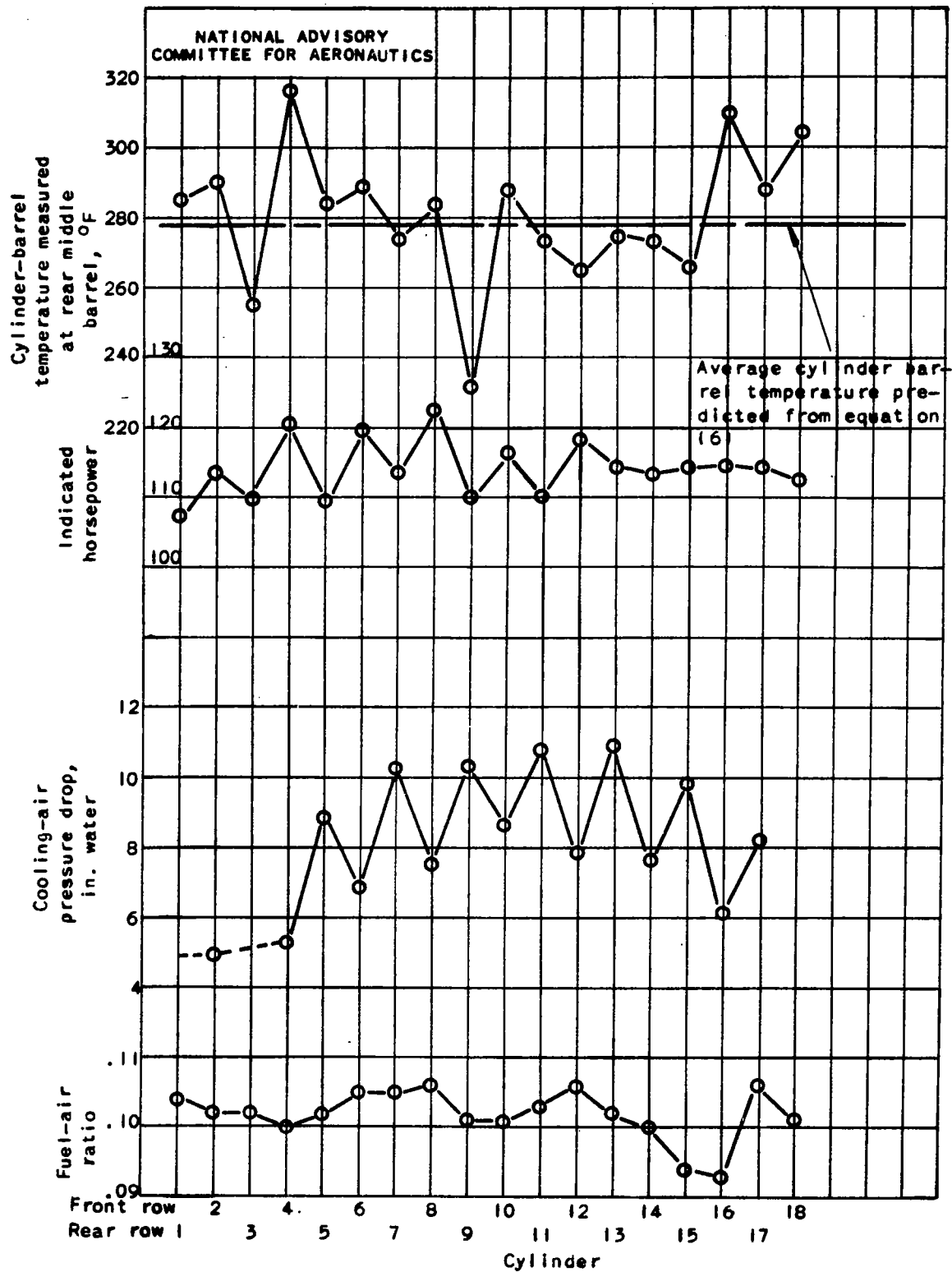


(c) Brake horsepower, 1500; engine speed, 2400 rpm.

Figure 11. - Continued.

Fig. 11d

NACA ARR No. E6C01



(d) Brake horsepower, 1700; engine speed, 2600 rpm.

Figure 11. - Concluded.

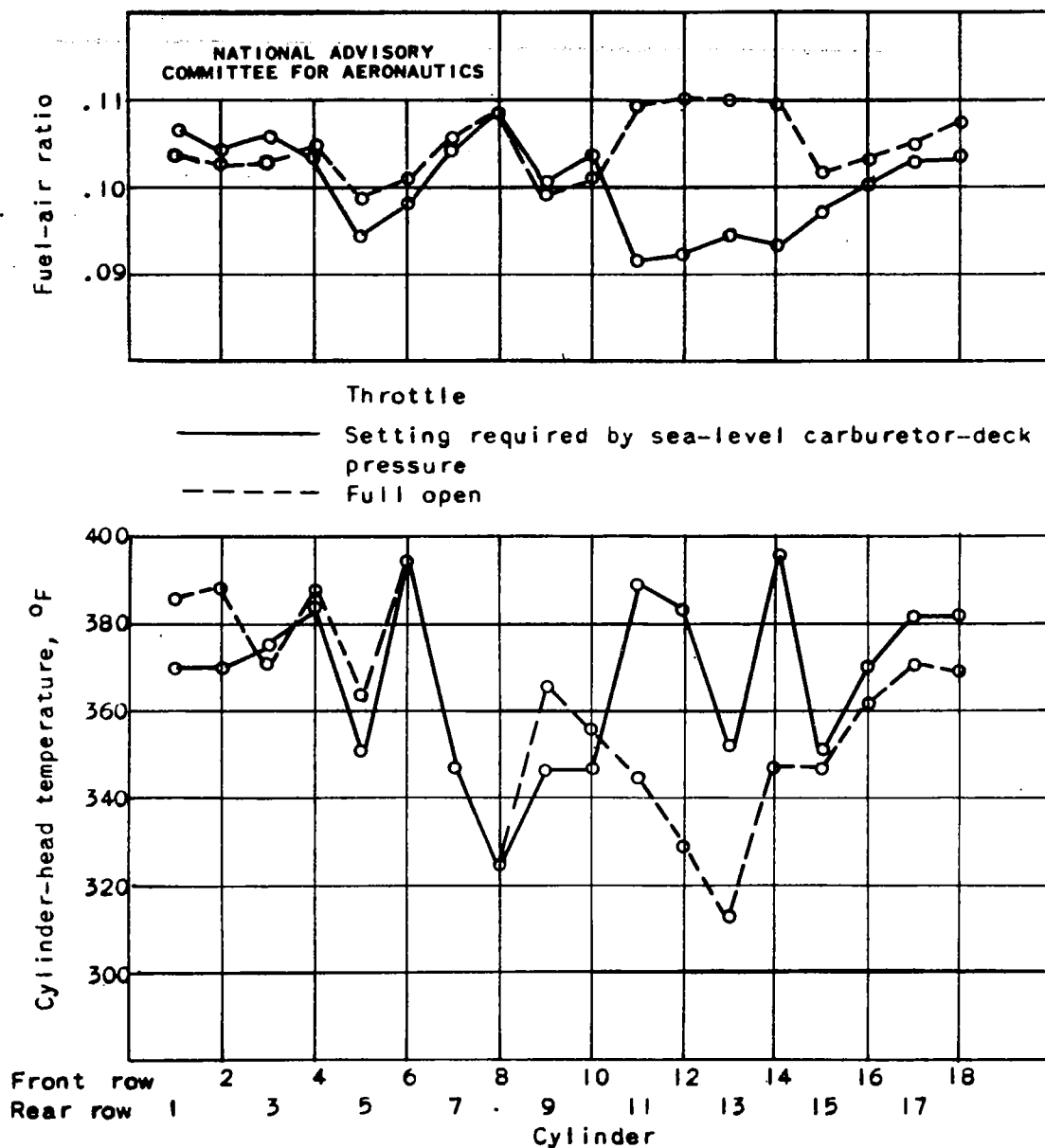


Figure 12. - Effect of throttle setting on mixture and temperature distribution. Supercharger in low-gear ratio; brake horsepower, 1000; engine speed, 2200; average fuel-air ratio, 0.103.

Fig. 13a

NACA ARR No. E6C01

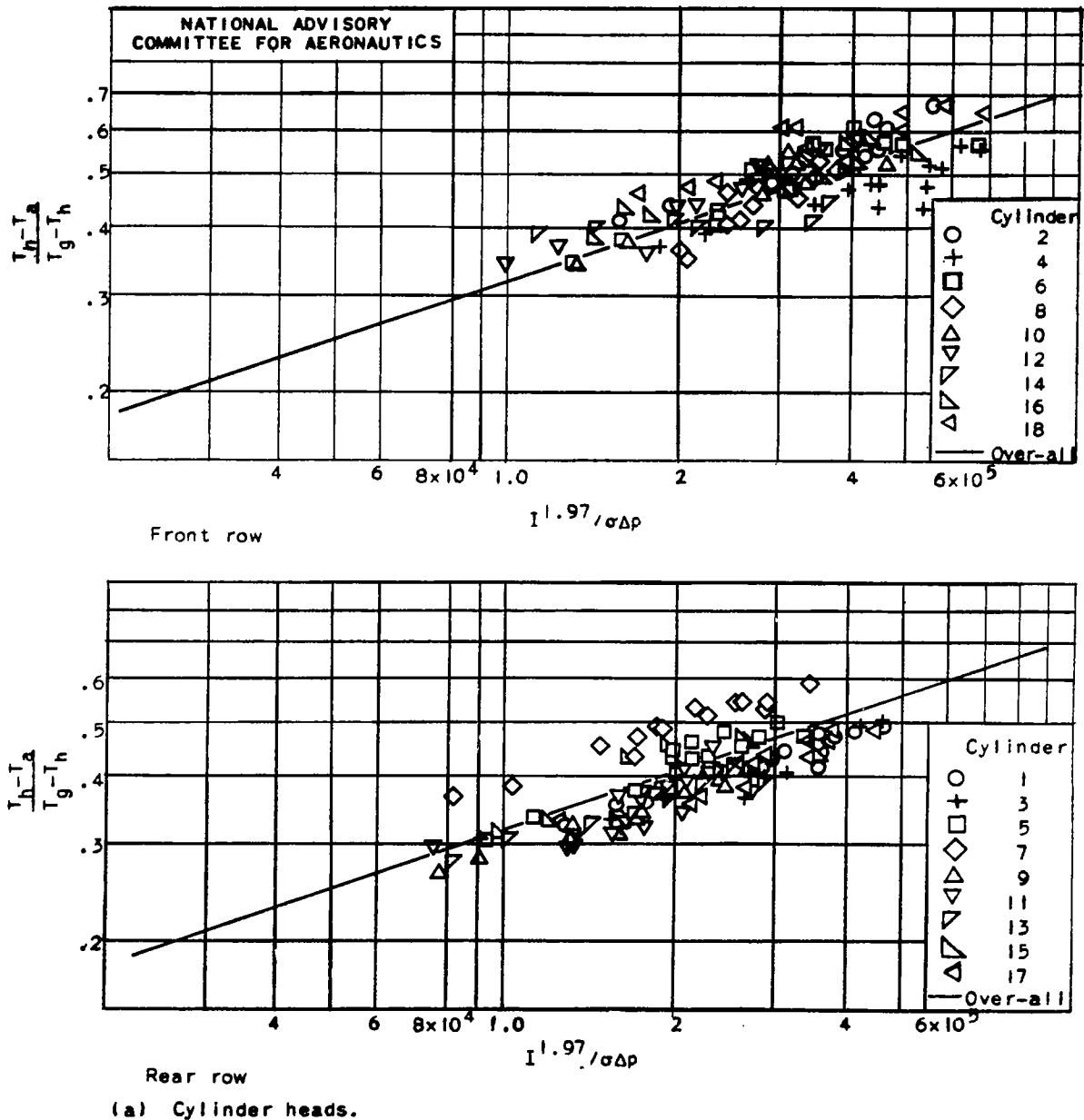
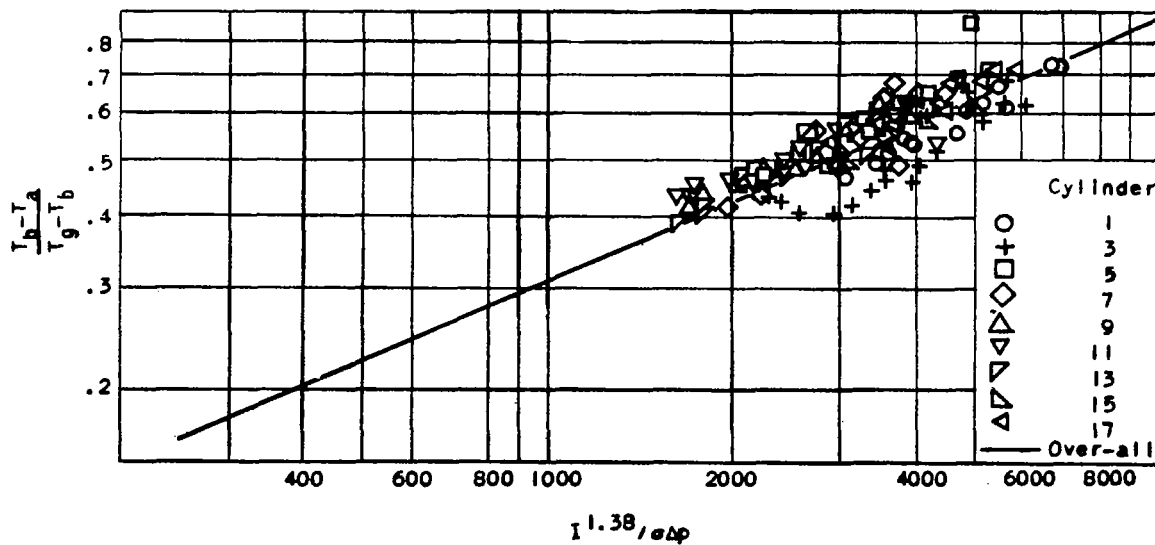
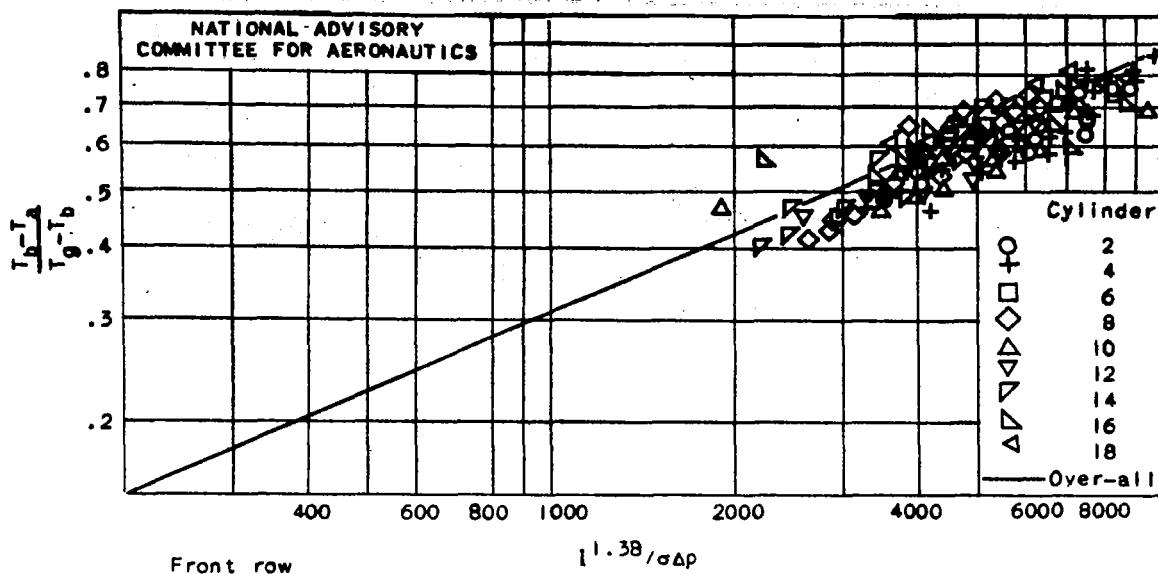


Figure 13. - Comparison of cooling data for individual cylinders with over-all cooling characteristics.



(b) Cylinder barrels.

Figure 13. - Concluded.

Fig. 14a,b

NACA ARR No. E6C01

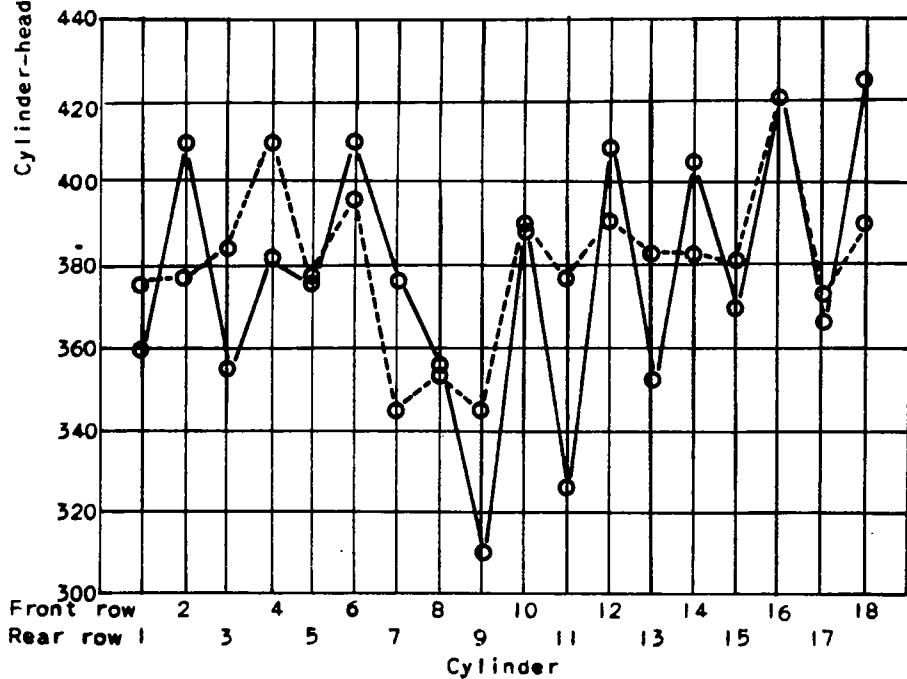
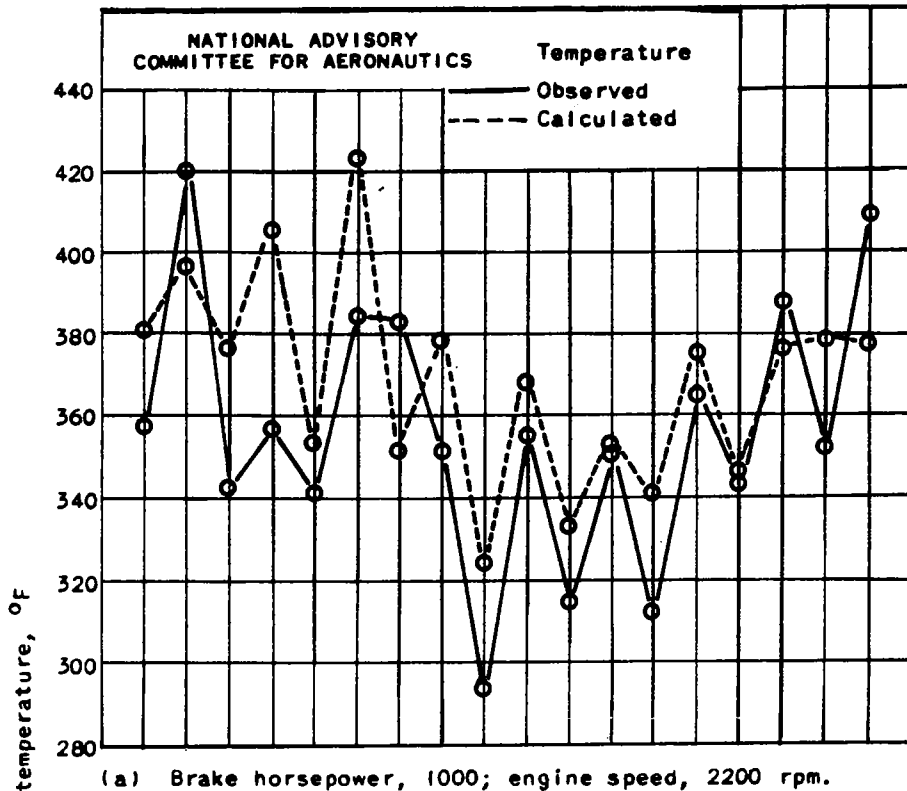
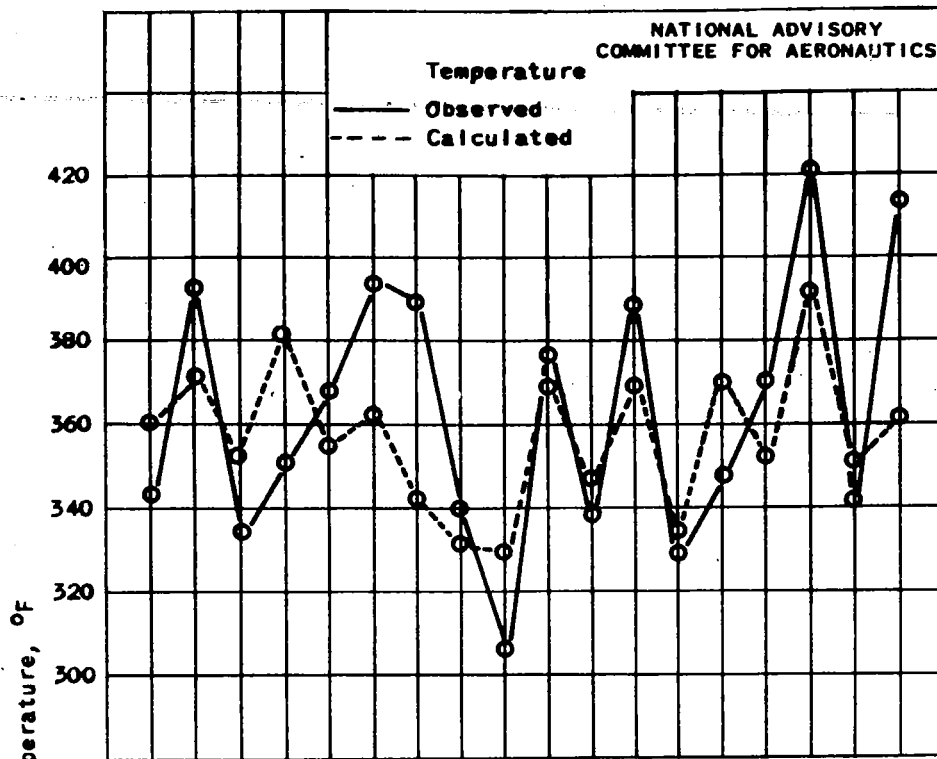
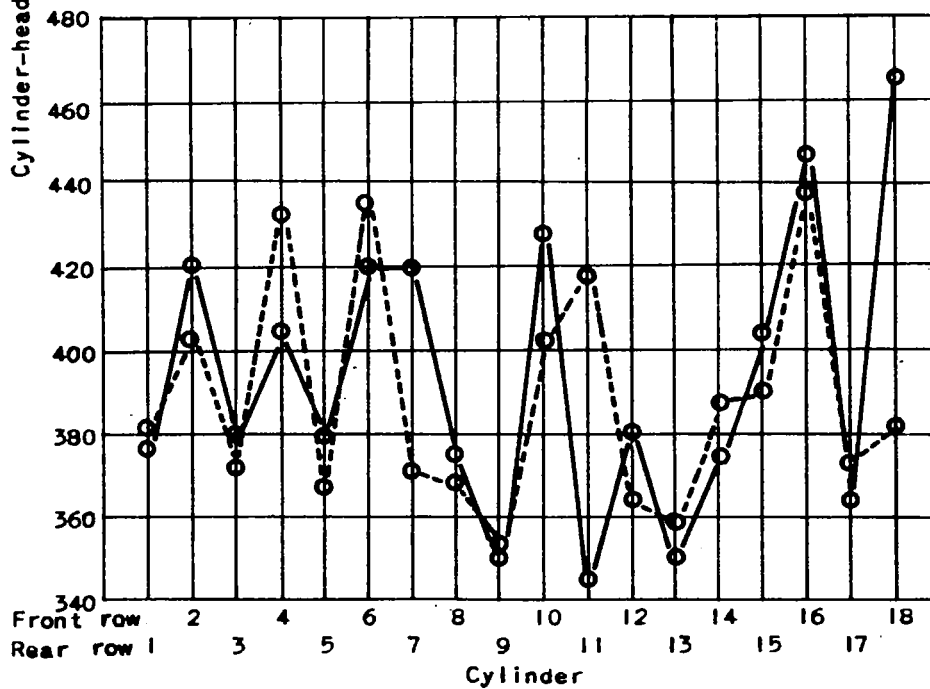


Figure 14. - Comparison of observed cylinder-head temperatures with head temperatures calculated from individual-cylinder operating conditions. Supercharger in low-gear ratio.



(c) Brake horsepower, 1500; engine speed, 2400 rpm.

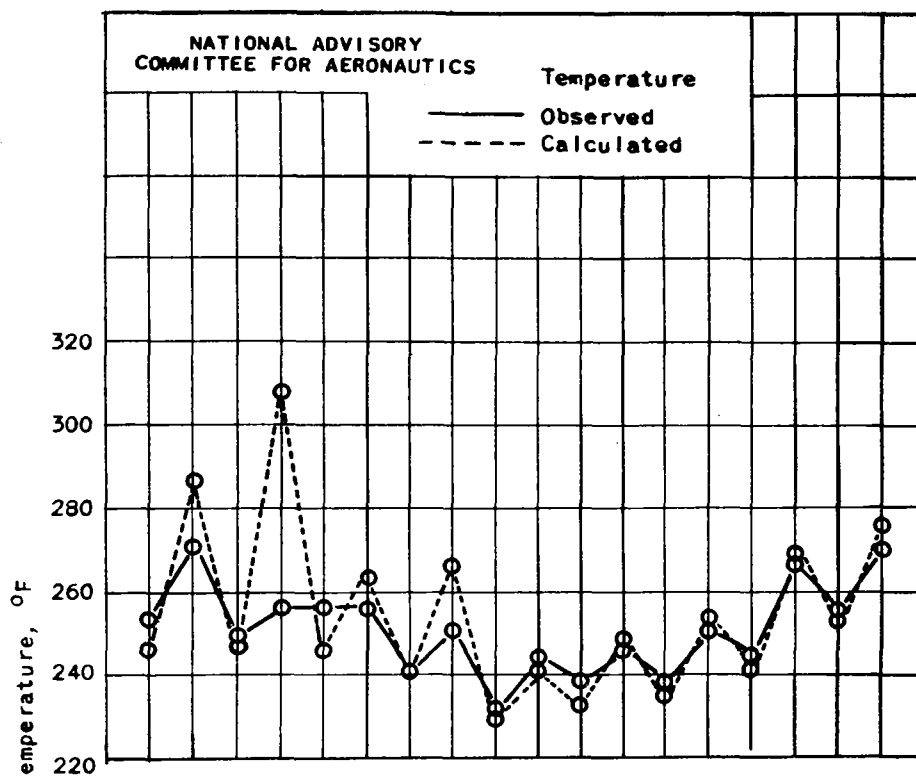


(d) Brake horsepower, 1700; engine speed, 2600 rpm.

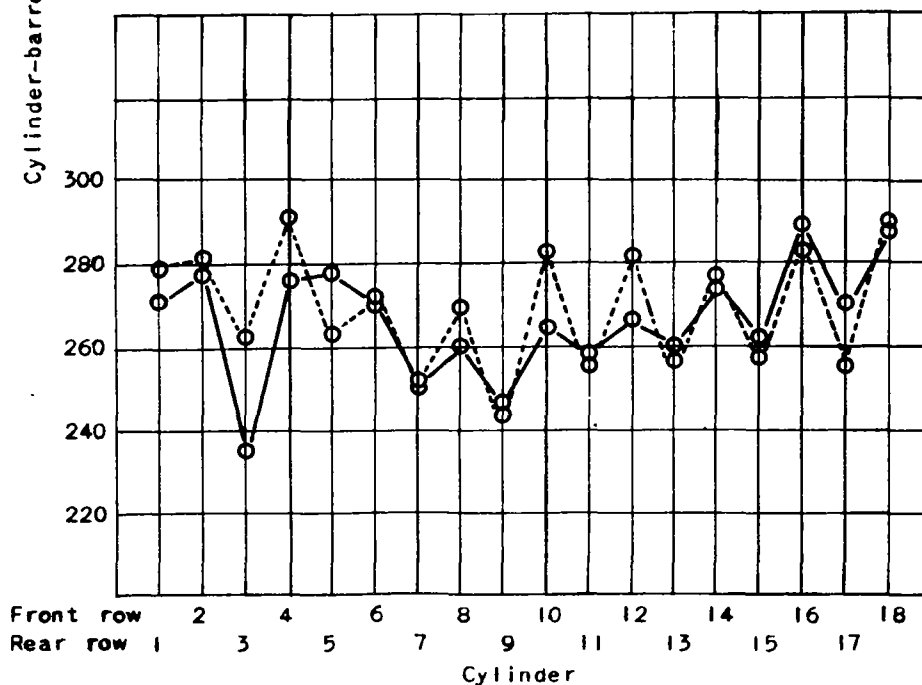
Figure 14. - Concluded.

Fig. 15a,b

NACA ARR No. E6C01

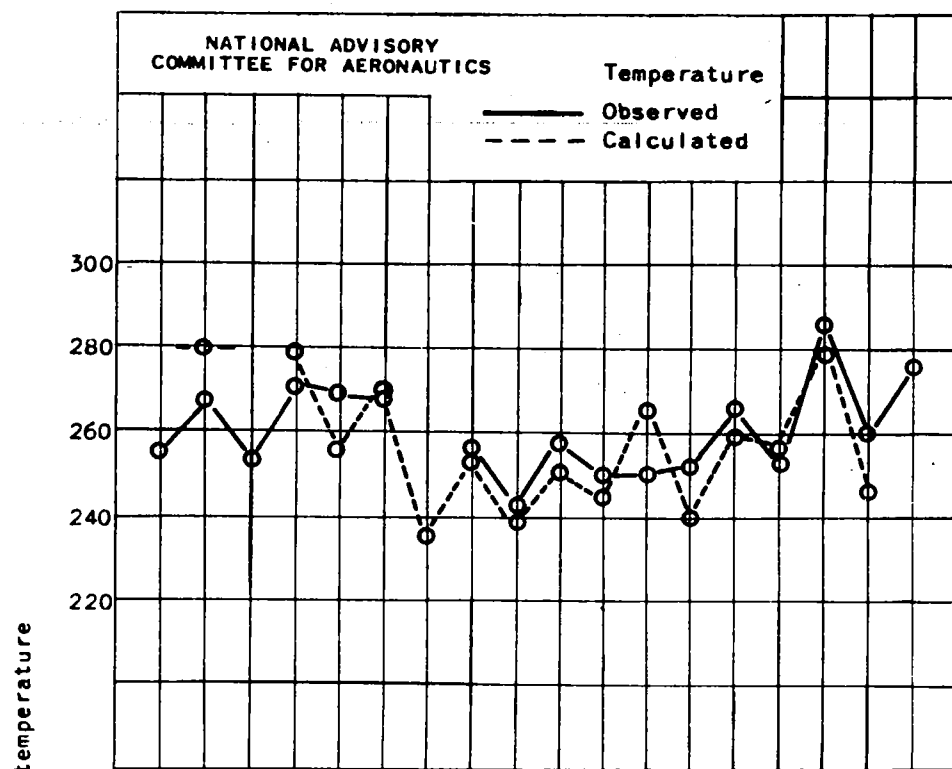


(a) Brake horsepower, 1000; engine speed, 2200 rpm.

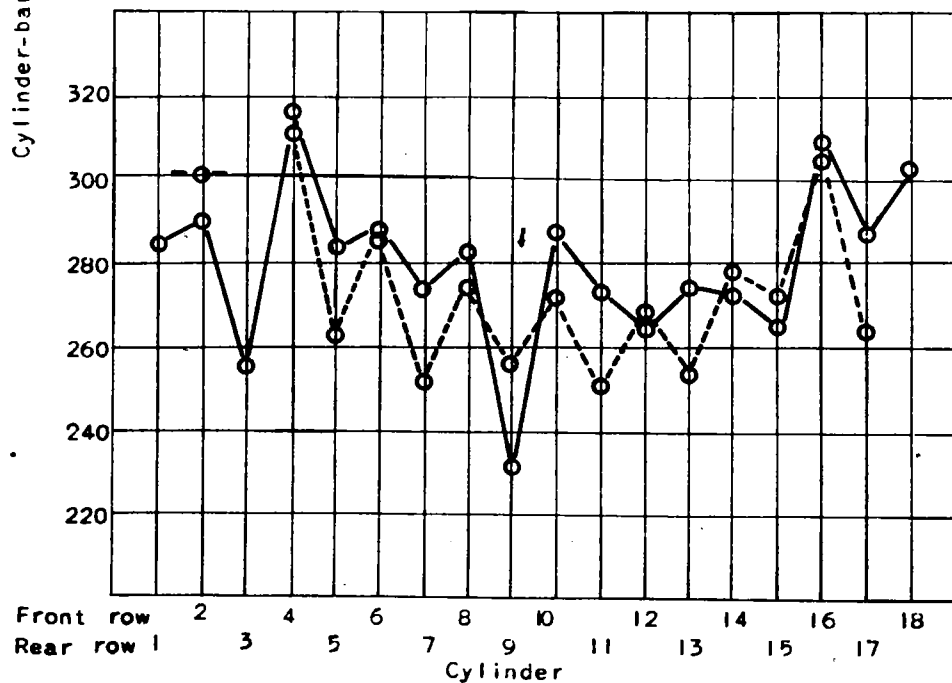


(b) Brake horsepower, 1400; engine speed, 2200 rpm.

Figure 15. - Comparison of observed cylinder-barrel temperatures with barrel temperatures calculated from individual-cylinder operating conditions. Supercharger in low-gear ratio.



(c) Brake horsepower, 1500; engine speed, 2400 rpm.



(d) Brake horsepower, 1700; engine speed, 2600 rpm.

LANGLEY RESEARCH CENTER



3 1176 01364 7608